THE ENERGY ANALYSIS OF ELECTRON BEAMS

by

Martin Gellender

A dissertation submitted to the Graduate Faculty in Chemistry in partial fulfillment of the requirements for the degree of Doctor of Philosophy, the City University of New York.

1976

This manuscript has been read and accepted for the Graduate Faculty in Chemistry in satisfaction of the dissertation requirement for the degree of Doctor of Philosophy.

2/2/76
date

Arthur D Baker
Chairman of Examining Committee

2/3/76
date

Leonard H. Schwartz
Executive Officer

Prof. Robert E. Kirby Robert E. Kirby
Prof. Robert Engel Robert Engel
Prof. Clyde Dillard Clyde Dillard
Prof. David Beveridge D Beveridge

The City University of New York

ABSTRACT

THE ENERGY ANALYSIS OF ELECTRON BEAMS

by

Martin Gellender

Adviser: Professor Arthur D. Baker

The rapid development of electron spectroscopy and related fields has introduced a new technology dealing with the generation, energy analysis and detection of electrons and other charged particles.

Many papers have been written investigating the resolution, transmission and other characteristics of particular energy analyzer configurations. Although energy analyzers have been compared and reviewed, a comprehensive overall outlook encompassing the limitations of performance of energy analysis systems has hitherto not been developed.

This thesis presents a general theory dealing with the fundamental principles of operation, and the limitations of performance involved in any attempt to energy analyze an electron (or charged particle) beam. The theory constitutes a distinctly new approach, capable of deriving general equations and conclusions applicable to all energy analyzers. In addition, some practical aspects of the production, focussing and energy analysis of electrons are discussed.

Table of Contents

LIST OF DIAGRAMS

LIST OF TABLES

I INTRODUCTION

In the last 50 years, experimental chemistry has undergone a metamorphosis brought about by the introduction of new instruments allowing the structure of atoms and molecules to be probed, yielding information inaccessible by earlier methods. The most dramatic developments during the first half of the twentieth century was the development of optical spectroscopy, whereby the spectrum of light radiation emitted, absorbed or scattered by a material allowed information about the electronic, vibrational and rotational states of the molecule to be determined. Atomic emission spectroscopy, absorbtion (with visible, ultraviolet and infrared radiation) and Raman spectroscopy, microwave absorbtion as well as NMR and ESR were developed as routine laboratory instruments. Although the various types of optical spectrometers may appear to be quite different, they share a common technology and have the same essential components: a source of radiation, a region where the radiation interacts with a material, a grating or prism to disperse the radiation of different wavelengths, and a detector.

Within the last two decades, a new type of instrumental technique has emerged - electron spectroscopy. In this form of spectroscopy, knowledge about chemical substances is gained by investigating the energy spectrum of electrons emitted, absorbed or scattered by the material. Although electron spectrometers have been constructed to serve a diverse range of functions, a technology has developed mutual to the various types of instruments. Since high vacuum is required (pressures at least below 10^{-5} torr) to prevent undesired interactions of electrons with air, the design of all electron spectrometers is

heavily influenced by the state of the art of high vacuum equipment. Furthermore, all electron spectrometers contain the same basic components: a source of electrons, a region where electrons interact with a material, an energy analyzer to disperse the electrons according to their energy, and an electron detector.

Fundamental to any electron spectrometer is the ability to energy analyze an electron beam. The device which performs this function, and is of crucial significance in the operation of the spectrometer, is termed an energy analyzer.

The operation of an energy analyzer is simplistically depicted in Fig.(1). Electrons of various energies are incident upon the entrance of the analyzer, which is "instructed" by a voltage applied to its internal electrodes to transmit only electrons of energy E_o. Ideally, the analyzer would transmit all electrons of energy E_o, while completely rejecting electrons of other energies.

Fig.(1)

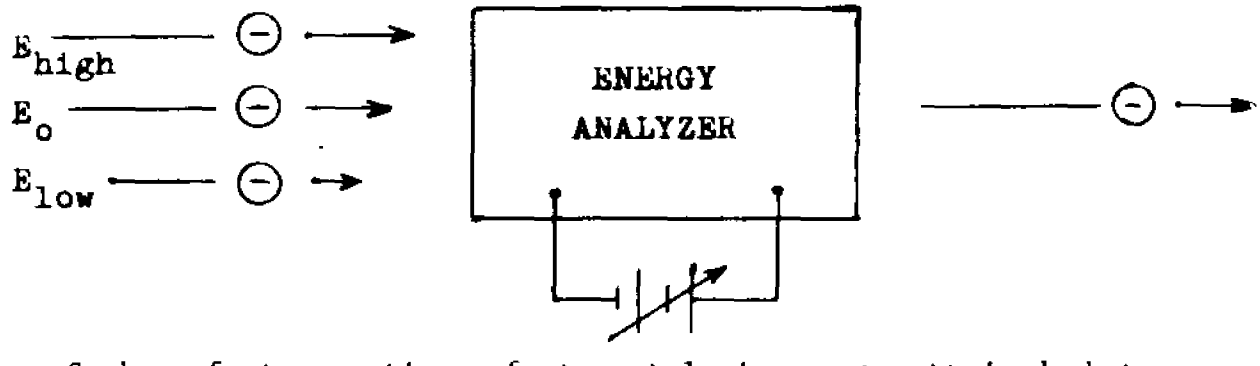

Such perfect operation unfortuneately is nev er attained, but serves only as a guide for the characteristics for which we should strive to approach. No analyzer ever provides infinite resolution of electron energies, but rather will transmit electrons within some

energy range ΔE. Consequently, the analyzer will not be able to discriminate completely between electrons differring slightly in energy if they are within the energy window of the analyzer, i.e., the range of energy ΔE transmitted by the analyzer.

Fig.(2) TRANSMISSION FUNCTIONS OF ENERGY ANALYZERS

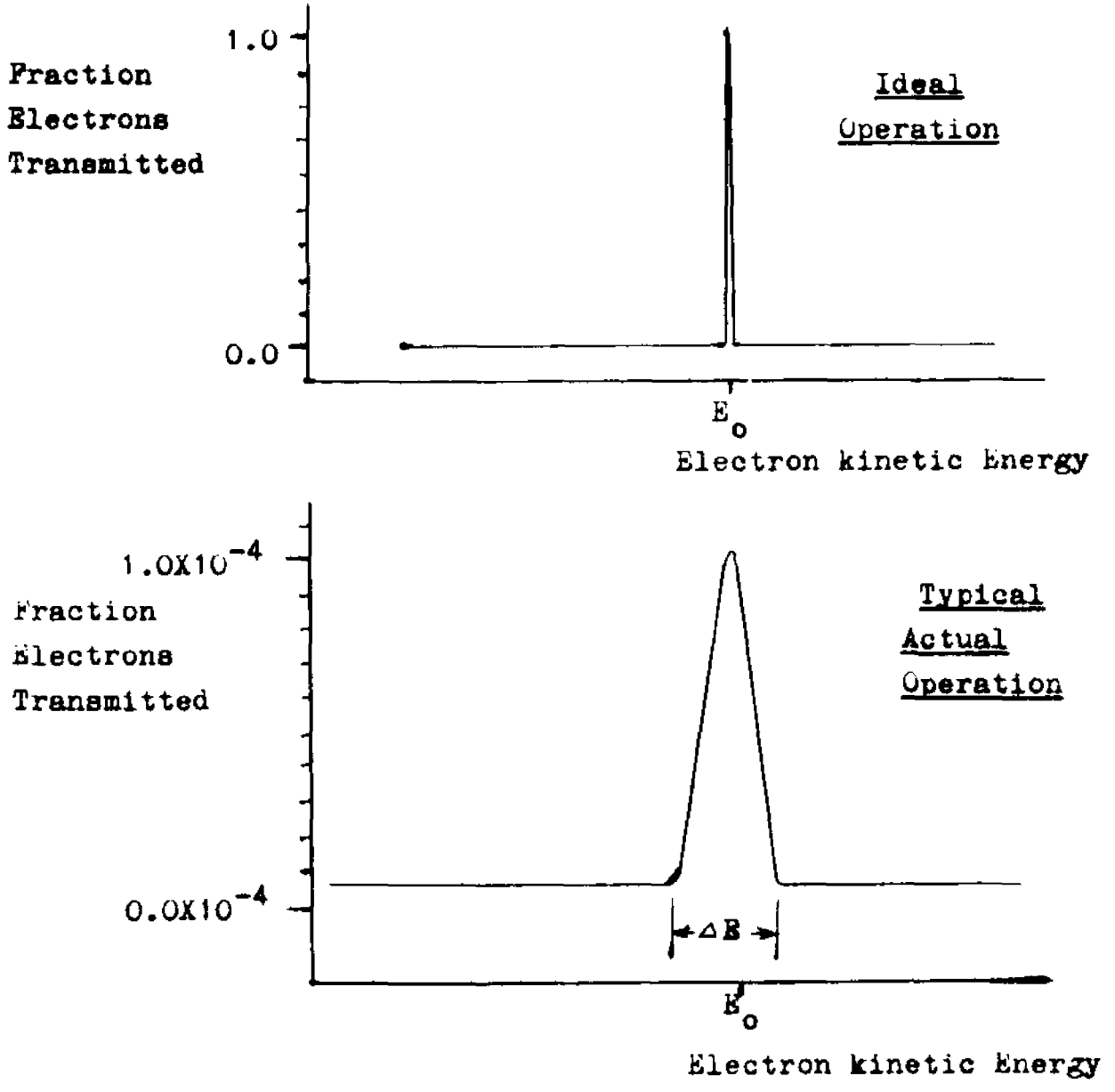

Ideally, all electrons with kinetic energies within the energy window of the analyzer should be transmitted, although in actual practice such operation is not even approached. As a requirement for high resolution, it is necessary to restrict electrons allowed to enter the analyzer to those within a small angular range. Typically, only about one electron in 10^4 will be within the proper angular range to be admitted into the analyzer: all others must be rejected, even if within the energy window of the analyzer.

Two conditions must exist for an electron to be transmitted by an energy analyzer.

(1) The electrons must be within the energy window of the analyzer.

(2) The electron must be within the proper angular range.

As higher resolution is sought, the angular range accepted into the analyzer must be compressed. As a consequence of high resolution then, the transmission of the analyzer will be very low for those electrons with the proper energy to be transmitted. In addition, high resolution will (by definition) compress the energy window of the analyzer, restricting electrons which can be transmitted to those within a narrower energy range.

Quite clearly, the attainment of high resolution is achieved at the expense of analyzer transmission. Considerable attenuation of electron beam intensity must therefore be expected whenever high resolution energy analysis is undertaken.

Since high resolution is always a desirable spectral characteristic enabling the maximum amount of spectral information to be derived, it might be suggested that if an energy analyzer were operated so as to provide very high resolution, the resulting low current of electrons transmitted by the analyzer and reaching the detector could always be compensated by an increase in amplifier gain. However, this is not the case. At the low current levels typically encountered in electron spectrometers (about 10^3 electrons/sec, or $2X10^{-16}$ amperes), the arrival of electrons at the detector must be viewed as occurring as distinct events, subject to statistical uncertainty-and noise. The noise source under discussion is not due to the limitations of available electronics, or thermal shot noise (although these may contribute additional noise), but rather a noise source intrinsic to the electron current being detected, due to random fluctuations in the arrival of electrons at the detector.

Perhaps the best way to illustrate this point, is to digress somewhat from the field of electron spectroscopy and consider a more mundane situation, although exactly analogous from a mathematical point of view. Let us consider an insurance company which insures 10,000 houses against attack by creeping jungle rot. Furthermore, let us presume that this affliction attacks houses entirely independently and randomly, and that the probability of any house being so destroyed in a period of one year (and thus requiring payment by the insurance company) is 1/100. It is then clear that in any year, the insurance company can expect to pay (10^4) (10^{-2}), or 100 clients. Recall however, that this affliction is a random event, and the number of houses destroyed in any particular year will probably not be exactly 100, but

rather follows a Poisson distribution. It is possible, for example, for the number of payments in a given year to be 86, 115 or 93. Upon investigating the number of payments made by the insurance company over a long period of time (see fig.(3)), it is interesting to note for each year how much the number of payments deviated from the expected value of 100. Over an extended (infinite) period of time, the annual fluctuations will average to a value of $(100)^{\frac{1}{2}}$, or 10 payments per year. For this case, or any situation where the outcome follows a Poisson distribution, if N events are expected to occur, the average deviation from the expected value will be $N^{\frac{1}{2}}$.

The arrival of electrons at the detector of a photoelectron spectrometer also follows a Poisson distribution. Consider for example, a photoelectron spectrometer in which 10^9 electrons are emitted from a material by photoionization. Only a very small fraction of these electrons will be transmitted by the analyzer and detected. The probability of an electron arriving at the detector would be of the order of 10^{-7}. Consequently, a signal of 100 electrons of some preselected energy E_o would be expected to arrive at the detector in a one second period. As fig. (3) demonstrates, this signal would not be constant, but would fluctuate, on the average, by 10 electrons/second. The detected signal may be thought of as containing two components: a constant, unvarying signal of 100 electrons/sec, and a random fluctuation-noise, averaging 10 electrons/sec. After detecting electrons for a period of one second, the noise component, which is of unknown value (although it will average 10 electrons over many one second measurements) will introduce uncertainty in the actual value of the signal due to electrons of energy E_o. To evaluate the limit

Fig.(3) Record of Payments to homeowners afflicted with (random) creeping jungle rot.

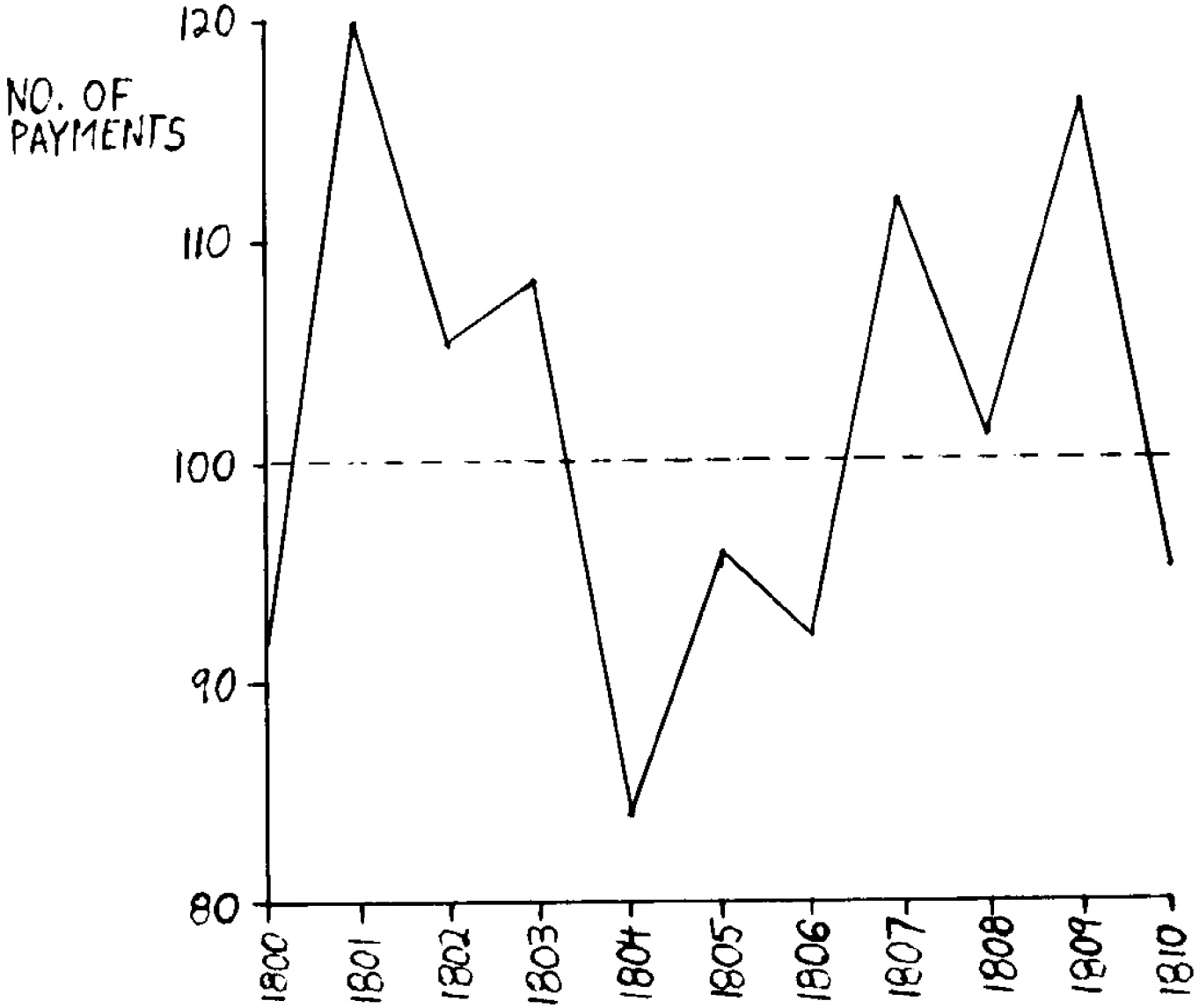

of confidence with which the spectral point may be regarded, a signal to noise (S/N) ratio of 10 would be assigned.

Only two recourses are readily available to increase the S/N ratio:

(1) increase the transmission of the energy analyzer, with an inevitable decrease in resolution, or

(2) collect electrons over a longer period of time.

An increase in the total time during which electrons of each energy are collected will lead to a larger number of detected electrons for each spectral point, and a proportionately lower statistical uncertainty in the signal. If a signal of s electrons/second is arriving at the detector, and electrons are counted for t seconds for a spectral point, then (st) electrons constitute the expected value of the data point. The statistical uncertainty in the signal is $(st)^{\frac{1}{2}}$, from which the S/N ratio for a pure signal is generally shown to be,

$$(I\text{-}1) \quad S/N = s^{\frac{1}{2}}t^{\frac{1}{2}}$$

Equation (I-1) is applicable only in cases where the detected electrons all constitute useful data, conveying information relevent to the chemical substance under investigation. However, some forms of electron spectroscopy, in generating signal electrons, inadvertantly produce a large background of electrons over a broad energy range. This is often the case for techniques in which a primary electron beam is used to excite atoms of the substance under investigation, which then eject electrons at discrete energies characteristic of the energy levels of the material (this is the case for example in Auger spectroscopy and negative ion resonance experiments). Invariably, some of

the incident exciting electrons will be scattered at various energies, providing a large background of electrons over the entire energy spectrum, an electron signal which provides no useful information about the chemical substance being studied. Such a background, which is often considerably larger than the actual signal, may readily be subtracted from the spectrum, as it contains no distinct variation with energy. Although the background remains essentially constant with energy and may be subtracted, the statistical fluctuations present in the background however cannot be predicted or subtracted, and inherently degrades the signal/noise of the real signal upon which it is superimposed.

For a signal of s electrons/second superimposed upon a background of B electrons/second, the average statistical uncertainty after collecting electrons for t seconds is $[(s+B)(t)]^{\frac{1}{2}}$, even after the background has been subtracted over the entire spectrum. The resulting S/N ratio is then,

$$(I\text{-}2) \qquad S/N = \left[\frac{s}{(s+B)^{\frac{1}{2}}}\right] t^{\frac{1}{2}}$$

From Eq.(I-2), it is possible to define the "effective rate of data collection", s_{eff}, as being the equivalent signal of pure data electrons which provides the same signal/noise ratio. Since Eq.(I-1) applies for such a signal, it follows that

$$(I\text{-}3) \qquad s_{eff} = \frac{s^2}{s+B}$$

As an illustration of how a large background degrades the statistical confidence of a signal, consider a real signal of 100 electrons/second superimposed upon a background of 1,000 electrons/second. The attainable signal/noise ratio would be equivalent to a pure signal of only 9 electrons/second.

It has been assumed here that the electrons reaching the detector are counted as distinct events. This is realized in actual practice, and the proliferation of digital electronics for use with electron multipliers has made digital counting techniques the generally accepted, and preferred, means of detection.

Virtually all electron spectrometers currently in operation utilize electron multipliers. An electron incident on the entrance of the multiplier will strike a surface, specially prepared to have a high yield of secondary electrons. The resulting secondary electrons ejected from the surface are accelerated to a kinetic energy of about 400 electron volts and strike another surface, whereby additional secondary electrons are produced, forming an avalanche effect as electrons are successively reaccelerated and collided with a suitable surface. An electron incident upon the entrance of the detector will typically produce an avalanche of about 10^8 electrons[1], constituting a current pulse lasting about 40 nanoseconds[2].

The output current from the electron multiplier may then be fed into a conventional picoammeter, producing an analog current proportional to the number of electrons incident on the electron multiplier. Such an analog detection system is generally not suitable for the detection of low electron count rates since it is susceptible to

various noise sources in addition to the inherent statistical noise in the signal.

Digital electronic counters, on the other hand, recognize and count the distinct current pulses generated at the output of the electron multiplier. Noise generated within the electronics itself is rejected unless it has the same amplitude and approximate waveform as the actual signal pulses. The use of digital electronic data counters is consequently much more suitable for the detection of low count rates (less than 10^6 per second[3]) of electrons, to a great extent eliminating all noise sources other than the intrinsic noise of the signal itself or noise associated with the electron multiplier[4].

At this juncture, the reader should now be well aware that any system employing electron (or ion) energy analysis will be characterized by two instrumental factors: energy resolution and rate of data collection. Since either of these performance characteristics may essentially be traded for the other, any consideration of an energy analyzer must consider both factors simultaneously.

The following chapters attempt to develop a general theory encompasing all energy analyzers, and the limitations of resolution and transmission which can be attained. The theory establishes a theoretical model of an energy analyzer and the performance which may be achieved under ideal conditions, at very high resolution. Before introducing the model, it would be advisable to dispel obvious criticisms.

The immediate response of an experimentalist to any theory generally is to query whether the theory is applicable to actual experimental conditions, or does it apply only to a hypothetical case. For example, the limitation of the velocity of light would be of little concern to a chariot driver in ancient Rome, who could more profitably focus his attention instead upon lubricating his axles. In electron spectroscopy however, the state of the art has progressed to the point where operation is often near the theoretical limit. With currently available equipment, there is no great gap of technology preventing experimentalists from approaching theoretical performance.

Furthermore, the theoretical limitations of electron energy analysis is only of relevance to experimentalists if achieving high resolution and data collection rates is a real restriction in the operation of electron spectrometers. Experimental work with x-ray[5] and ultraviolet photoelectron[6] spectrometers by the author and coworkers has clearly confirmed that in actual practice, obtaining high resolution spectra often requires a considerable period of data collection. Particularly an investigation of the bonding of metal ions in protein molecules[5] often required several hours of data collection before yielding an unambiguous spectrum. Coincidence experiments involving electron energy analysis (see chap. 6 of this thesis), which are capable of yielding information directly accessible through no other technique, currently require days of data collection to obtain moderate resolution spectra with satisfactory signal/noise ratios.

As the limitations of analyzer transmission are generally only of consequence at high resolution, and as the further development of electron spectrometers will no doubt be aimed at obtaining higher resolution, the theory restricts its scope to the condition of high resolution.

II ENERGY ANALYZERS: AN OVERVIEW

All energy analyzers have certain general features in common, function in essentially the same way, and are subject to the same limitations. Therefore, rather than consider each type of analyzer (differing in geometric configuration of electrodes) as a separate entity, it is useful to consider energy analyzers in a very general way, referring to specific energy analyzers only for illustrative purposes.

In any experiment, in which electrons are to be energy analyzed, a source of electrons must be present. The electrons almost always originate from within a low pressure gas, or the surface of a solid. It is assumed that the electrons eminate from the source with discrete energies at all angles over the area of the source.

To attain high resolution, it will be necessary to limit access into the analyzer only to electrons originating from a small area and within a small angular range. This function is generally accomplished by several entrance slits. A slit defining the area of the electron beam entering the analyzer is termed a window (adopting the terminology of light optics), wh ile the slit limiting the angular divergence of the incident beam is termed an aperture, or pupil. The entrance slits consequently form a well collimated beam by rejecting all electrons outside of the desired area and angular range. Of course, the more collimated is the beam passed by the entrance slits, the greater will be the fraction of source electrons which are rejected by the entrance slits. The rejection of source electrons required to achieve high resolution will be a fundamental limitation of the performance of the analyzer.

The well collimated beam of electrons accepted by the entrance slits enters an electron optical dispersive element, identical in function to a prism in light optics. The dispersive element may employ electrostatic or magnetic fields to deflect the electron according to its kinetic energy. Although the following discussion will be limited to electrostatic analyzers (as these have become the preferred type, being almost universally accepted for recent commercial and research spectrometers), it is expected that a similar consideration of magnetic analyzers would yield identical results.

Although the dispersive element may vary considerably in physical form, utilizing parallel plates[7], cylindrical plates[8], concentric spherical sections[9], concentric cylinders[10,11] or conceivably almost any geometric shaped electrodes establishing a well-defined electrical potential, the purpose is always to deflect the electrons according to their energy. Electrons leaving the dispersive element are projected upon an image plane so that an electron will strike the plane at a position corresponding to its energy. In order to select electrons of one particular energy, a slit in the image plane will allow electrons of that preselected energy to be transmitted.

Two basic characteristics of an energy analyzer must be considered. The first feature, which is highly desirable, is a high energy dispersion of the analyzer. In other words, electrons differing only slightly in energy should be widely separated on the image plane.

The second feature, which degrades the performance of the analyzer and limits the attainable resolution, is the aberration of the analyzer. Ideally, all electrons of the same energy should be focussed to precisely

the same point in the image plane. However, due to imperfect collimation of the beam by the entrance slits, electrons of the same energy entering the dispersive element at slightly different angles, or entering at a slightly different point in the entrance window, will be focussed onto a smeared area on the image plane.

The Parallel Plate Analyzer

As an illustration of the operation of an energy analyzer, consider the parallel plate analyzer. Although this analyzer has not been employed extensively in recent research and commercial electron spectrometers, its rudimentary electrode configuration greatly simplifies mathematical analysis.

It is generally appreciated that two parallel plates, across which is applied an electrical voltage, will establish a uniform electric field in the region between the plates. This is strictly true however, only for electrodes of infinite extent, otherwise fringing effects distort the electric field near the outside edge of the electrodes. In order to achieve a uniform electric field within the region between the two plates, as is required in subsequent calculations, three recourses are possible.

(1) The plates may be made much larger than the spacing between the plates.

(2) Electrodes may be placed around the outside of the constant field region, to which suitable potentials are applied as to hold these regions of space at the same potential as would exist if the plates were infinite in size

(3) The problem may be ignored.

While ignoring the problem of fringing effects may appear to be a blatant disregard for the laws of physics, apparently this approach may be applied (and often is), without adverse degradation of performance. This is probably not due to the effect of fringing being of small consequence, but due rather to the nearly equal effect of fringing fields upon electrons of similar energy. The effect of fringing then is essentially to shift all electron trajectories to the same extent, while leaving unchanged the ability of the analyzer to disperse electrons of different energies.[12]

Fig.(4) The Parallel Plate Analyzer

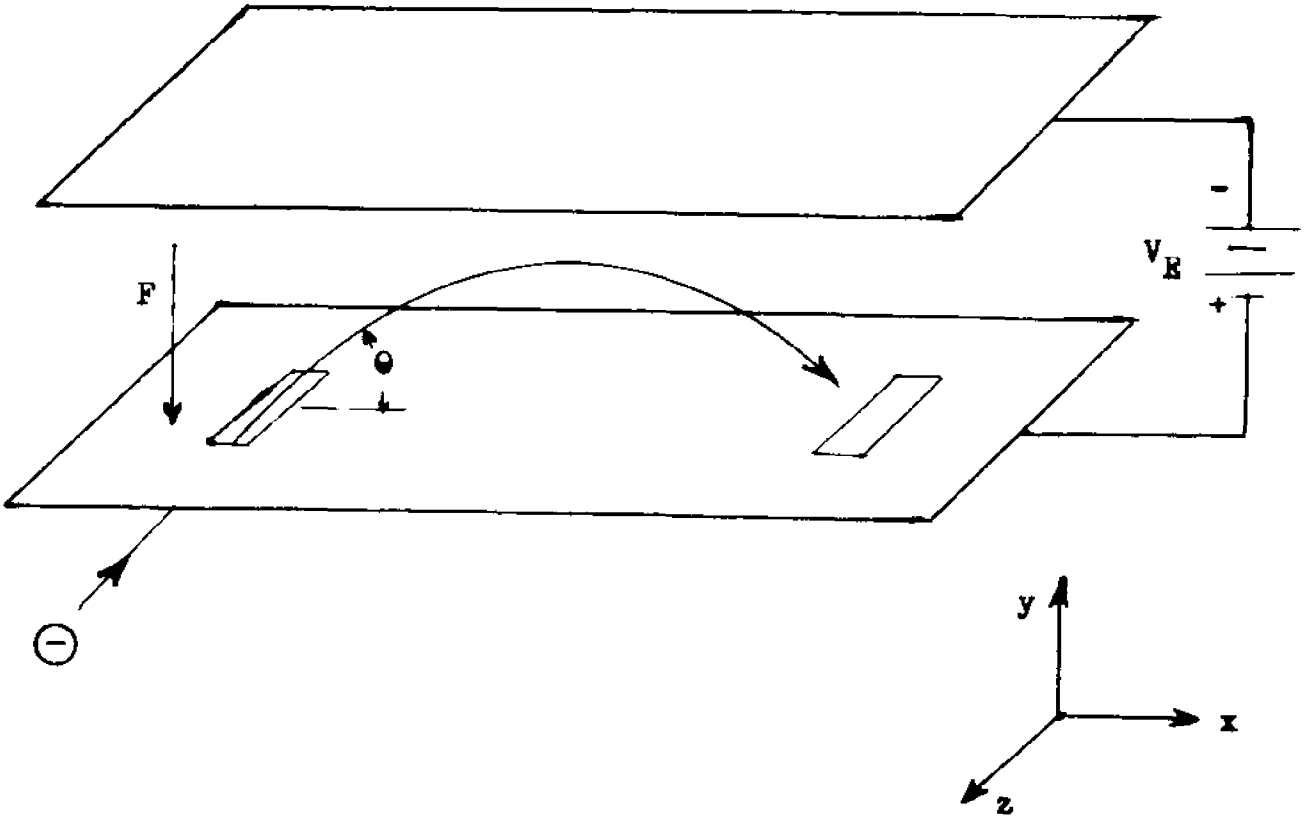

In any event, we consider here the trajectory of an electron of kinetic energy E upon passing through a slit in one plate and entering the constant field region (see fig.(4)). Upon entering the region between the two plates, the electron will experience a constant force F which will (if the polarity of the voltage applied to the plates is correct) repel the electron back toward the plate from which it entered the region. When the electron returns to the electrode surface, the distance traveled along the length of the plate will depend directly upon the kinetic energy at which the electron entered, thereby allowing electrons of different kinetic energies to be dispersed.

The parabolic electron trajectory is exactly the same as experienced by a cannonball subject to the constant gravitational field of the earth. A vertical component of velocity maintains the projectile in flight for some time duration, while the horizontal velocity component-acting independently - carries the projectile some horizontal distance during the time that the projectile is maintained in flight. The greater the energy at which the cannonball is launched, the further will be the horizontal distance traveled.

The kinetic energy of the electron (or cannonball) is not however the only factor which determines the distance traveled by the electron along the length of the electrode plate. In addition, the angle at which the electron enters the analyzer determines to a great extent the distance traveled, and it is highly desirable to introduce a focussing property which minimizes this effect.

Envision the electron to emerge into the constant field region at an angle θ with respect to the electrode plate. The velocity of the

electron may be resolved into two independent velocity components, v_y in the direction perpendicular to the electrode surface (vertical) and v_x in the direction parallel to the electrode surface (horizontal). As force F is exerted upon the electron perpendicular to the electrodes, the electron will be decelerated in the y direction until the y velocity component is zero, and then will be reaccelerated back to the electrode plate. Applying the well-known Newtonian equations of motion, it is straightforward to calculate the time that the electron is maintained in flight by the v_y velocity component.

Since $F=m_e a$ (where m_e is the mass of an electron, and a is the electron acceleration), and $v_y=a \cdot t$, then the total time t that the electron remains in flight between the plates is,

$$t=2m_e v_y/F \qquad \text{(II-1)}$$

During this time duration, the velocity component v_x remains constant and translates the electron in the direction along the electrode surface. The total distance traveled by the electron in the x direction in the course of its trajectory, S, is

$$S = V_x . t$$

$$S = 2m_e v_x v_y/F \qquad \text{(II-2)}$$

Elementary vector analysis provides the magnitude of velocity components v_x and v_y in terms of angle θ and the total velocity v of the electron.

$$v_x = v\cos\theta \qquad \text{(II-3)}$$

$$v_y = v\sin\theta$$

Substituting these relationships into Eq. (II-2) provides an equation relating the distance S traveled by the electron in terms of

its kinetic energy E, and the angle at which the electron enters the analyzer.

$$S = 2m_e(v\cos\theta)(v\sin\theta)/F = 4(\tfrac{1}{2}m_e v^2)\cos\theta\sin\theta/F$$

$$S = 4E\sin\theta\cos\theta/F \qquad \text{(II-4)}$$

It is desired to focus electrons only according to their energy, and not according to the angle of entry into the analyzer. Such a focussing property is achieved, to a first order approximation, under the condition where $dS/d\theta = 0$. Differentiating Eq.(II-4) to obtain the condition for such a first order focussing property,

$$dS/d\theta = (4E/F)(\cos^2\theta - \sin^2\theta) = 0 \qquad \text{(II-5)}$$

$$\theta = 45^o$$

Thus, if the angle of entry into the analyzer is restricted to within a small angular range centered about 45^o, the distance S traveled by the electron before striking the electrode plate depends linearly upon the kinetic energy of the electron, and not upon the angle of entry into the analyzer. Upon inserting an exit slit in the electrode plate at some distance S_o from the entrance slit, electrons entering the analyzer at a kinetic energy of $FS_o/2$ will be transmitted through the exit slit of the analyzer. The electron kinetic energy transmitted by the analyzer may be varied by altering the voltage V_E applied between the electrode plates (since $F = V_E/d$, where d is the distance between the plates). The kinetic energy of the electrons transmitted by the analyzer will then be proportional to the applied voltage.

$$E = \tfrac{1}{2}(S_o/d)V_E \qquad \text{(II-6)}$$

When it is desired for the kinetic energy of the electrons (measured in electron volts) transmitted by the analyzer to be numerically equal to the voltage applied across the plates, a convenient but not necessary condition, the analyzer may be constructed as to satisfy the relationship that $\frac{1}{2}(S_o/d) = 1$, i.e., the distance between entrance and exit slits is twice the plate separation.

The foregoing discussion has demonstrated that, using parallel plate electrodes, it is possible to achieve dispersion of electrons according to their energy, allowing high resolution energy analysis. This should not be construed to imply that ideal energy analysis is thereby at hand - for it has been assumed that only electrons within a very narrow angular range are to be accepted into the analyzer. The independence of the distance S traveled by the electron along the image plane (in this case, the electrode plate) from the angle of entry into the analyzer is only a first order approximation, which fails quite miserably at angles deviating considerably from 45^{o}. An attempt to accept a large angular range into this analyzer will inevitably degrade the ability of the analyzer to resolve electrons of slightly different energies.

The inability to focus monoenergetic electrons to the same point in the image plane, originating from the angular range of electrons entering the analyzer, is termed the angular aberration of the analyzer. Due to non-ideality of the focussing, the parallel plate analyzer is subject to exactly twice the angular aberration of other common first order focussing analyzers. It is therefore worthwhile to consider briefly an analyzer more typical of first order operation

(and one which has been extensively applied in VUV Photoelectron Spectroscopy[13]), the 127° cylindrical sector analyzer.

The Cylindrical Sector Analyzer

The electric field between two infinitely long concentric cylinders of radii R_I and R_O across which a voltage V_E is externally applied may readily be calculated from Gauss's law. An electron in the region between the concentric cylinders at radius R will experience a force F_R accelerating the electron inward toward the axis of the cylinders. It has often been stated[8,14] that

$$F_R = \left[\frac{V_E}{\ln(R_O/R_I)}\right] /R \qquad \text{(II-7)}$$

As shown in Fig.(5), a cylindrical sector analyzer basically consists of two concentric cylindrical sectors. Except at the two ends of the sector, where fringing effects may be significant, the electric field between the cylindrical electrodes would be expected to be the same as the field between two complete cylinders of infinite length, given by Eq. (II-7). A slit near one end of the sector allows electrons to enter the field at radius R.

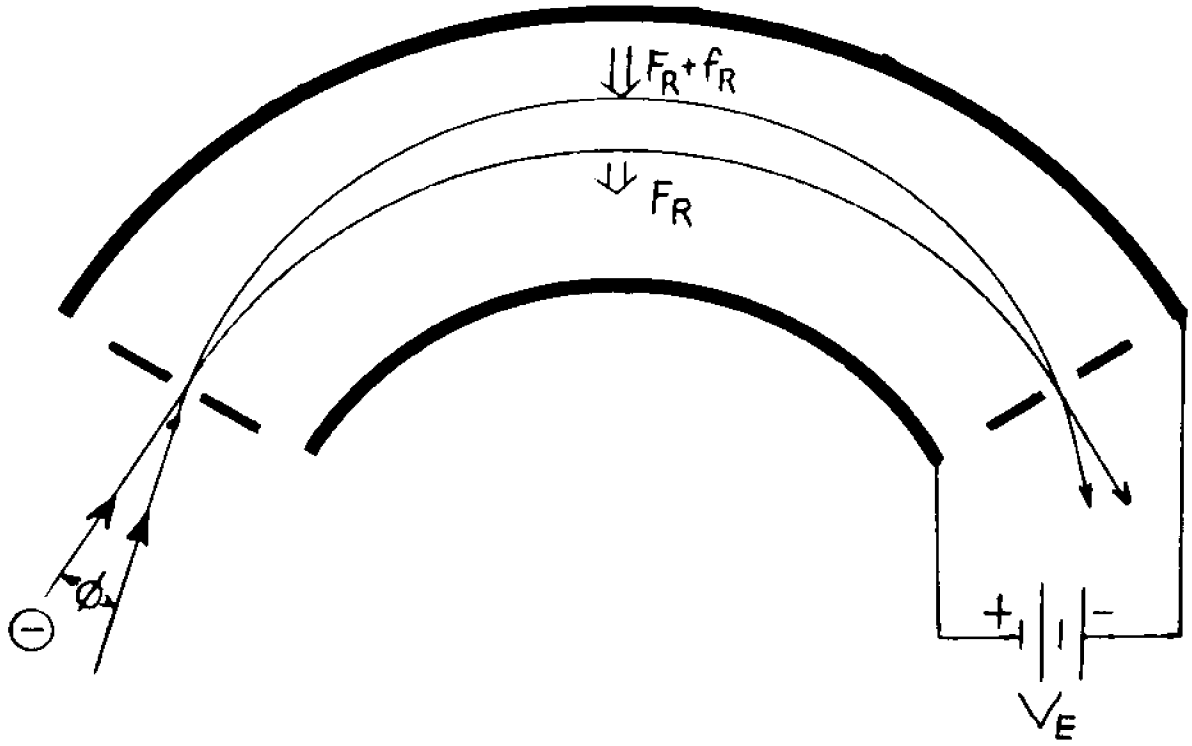

Fig.(5) The Cylindrical Sector Analyzer

If an electron of velocity v were to pass through the entrance slit and be projected tangentially into this field at radius R, the electron would be maintained in a circular trajectory if the radial force F_R provided the centripetal acceleration required to maintain the electron in a circular trajectory. This condition may be mathematically stated as

$$F_R = m_e v^2/R \qquad \text{(II-8)}$$

It is clear that this geometry is capable of energy analyzing an electron beam, since only electrons of one kinetic energy ($\frac{1}{2}m_e v^2 = \frac{1}{2}RF_R$) will be maintained in a circular trajectory at radius R and be transmitted through an exit slit at this radius at the other end of the

sector. Electrons of other kinetic energies will be radially deflected. If it is desired that the kinetic energy of the transmitted electron (in units of electron volts) be numerically equal to the voltage V_E applied across the plates, then application of Eq.(II-7) shows that this condition is met when $R_o/R_I = e^{\frac{1}{2}} = 1.65$.

An electron entering the entrance slit of the analyzer tangentially with the proper energy to be maintained by the electric field in a circular trajectory of radius R is termed the central-ray trajectory. This will be a convenient reference trajectory since it is at the center of the angular range accepted into the analyzer. Of course, most electrons will not enter the analyzer exactly tangentially, but rather will be incident on the entrance slit at some angle ϕ relative to the central ray trajectory. In order to achieve the maximum resolution, it is necessary for a focussing condition to exist such that all electrons of the same energy should be focussed to the same point by the exit slit - regardless of the angle ϕ with which an electron enters the analyzer.

Clearly, an electron entering the analyzer at an angle ϕ from the central ray trajectory (as shown in Fig.(5)) will follow an alternate trajectory, which will carry the electron to greater radial distances, until eventually it converges with the central ray trajectory. The fact that the two trajectories will converge, at a point independent (to a first order approximation) of the angle of entry ϕ, implies that there exists some effective force acting on the electron in an alternate trajectory in addition to the force F_R experienced by the central ray electron. A somewhat detailed mathematical analysis[15] shows that this effective force pushing the alternate ray electron towards the central ray trajectory, f_R,

is proportional to the separation, r, between the two trajectories.

The effective force f_R arises as a net consequence of four effects.

(1) An electron at a greater radial distance than the central ray trajectory will be of lower kinetic energy and hence will be accelerated inward to a greater degree than the central ray trajectory.

(2) The alternate ray electron will travel in a longer trajectory and consequently be exposed to force F_R for a greater period of time.

(3) The greater radius of the alternate ray electron requires less centripetal acceleration to maintain the trajectory.

(4) At larger radial distances, the value of F_R will be decreased (acting in opposition to the other three effects).

The net result of this analysis is that

$$f_R = \left[\frac{F_R^2}{dE} + \frac{dF_R}{dR}\right] r \qquad \text{(II-9)}$$

where E is the kinetic energy of the electron.

Since the effective restoring force is directly proportional to the separation from the central ray trajectory, f_R acts as a harmonic restoring force so that the separation from the central ray trajectory varies sinusoidally with time. The oscillation of the distance from the central ray trajectory has a characteristic half period, after which all electrons will converge, independently of angle Ø.

Upon making the proper substitutions and manipulations of Eq.(II-9), it is possible to demonstrate that the electric field of the cylindrical sector analyzer results in a relative restoring force, f_R, of $(F_R^2/E)r$, so that (F_R^2/E) constitutes the force constant of the oscillation. The separation of the electron paths from the central ray trajectory oscillates

with a half period of $\pi R/2^{\frac{1}{2}}v$. A focussing point then results at a distance along the trajectory of $\pi R/2^{\frac{1}{2}}$, requiring the sector field to subtend an arc of $\pi/2^{\frac{1}{2}}$ radians, or $127^{o}17'$.

It is useful to consider the velocity of the electron incident upon the analyzer entrance slit as having two independent components: v_{cr} parallel to the central ray trajectory, and v_p perpendicular to the central ray trajectory, where

$$v_{cr} = v\cos\phi$$

$$v_p = v\sin\phi$$

Due to the focussing condition achieved at a sector angle of 127^{o}, the energy associated with the velocity component perpendicular to the central ray trajectory will have no bearing on the final point of impact of the electron trajectory on the image plane. As a general statement describing the characteristics of optimal focussing in all first order focussing analyzers, it may be generalized that the position S at which an electron strikes the image plane depends only upon the energy component along the central ray trajectory, that is,

$$S = kE\cos^{2}\phi \qquad \text{(II-10)}$$

where k is an analyzer constant, E is the electron kinetic energy, and ϕ is the deviation of the entry angle from the central ray trajectory.

Although first order focussing analyzers vary considerably in electrode configuration and electric field geometry, the performance which is theoretically attainable is essentially identical. The reasons for this surprising result is that the operation and focussing of first order energy analyzers are basically the same.

The inability of an analyzer to focus all electrons of the same energy to the same point in the image plane, due to the finite angular acceptance range, will result in the failure of the analyzer to completely discriminate between electrons of nearly the same energy. High resolution then, may be achieved by restricting the angular acceptance range of the analyzer to a very narrow span by means of an electron optical system (in simplest form consisting of several slits), allowing high resolution to be attained at the sacrifice of transmission. The limitations of electron energy analyzers lie not only in the focussing characteristics of the electrode geometry, but also in the shortcomings of the entrance electron optical system.

Perhaps, as one may suppose, the entrance optics could consist of a series of electron lenses designed to focus all electrons from the source to within a very narrow angular range. That would allow virtually all electrons from the source with the proper energy to be transmitted by the analyzer, while allowing high resolution to be achieved. Such an experiment, incorporating the most ingenious electron focussing techniques, would be doomed to failure. Why could an electron optical system not be constructed so as to focus electrons from the source into a perfectly collimated beam? The answer is that electron optical laws (based on either statistical or thermodynamic considerations) limit the ability of any focussing system to form a collimated beam. The only means always available of increasing the collimation of the beam is to reject a greater fraction of the source electrons. While this option will allow higher resolution to be attained, the number of electrons transmitted by the analyzer will be decreased substantially. In order to achieve high resolution, energy analyzers are commonly designed so that about 10^4 electrons

of the proper energy will be rejected for each electron transmitted by the analyzer.

Perhaps the reader is puzzled by the fundamental futility of attempting to increase the beam brightness (electron current/unit area, unit solid angle) by a clever design of an electron optical system. This restriction can be illustrated more readily in light optics, where a similar law applies.

Consider the well known ability of a magnifying glass to focus rays from the sun onto a small spot, thereby developing very high temperatures at a small area. Since rays from the sun are nearly parallel at the surface of the earth, light rays will be focussed onto the focal point of the lens. By using a superb, aberration-free lens, employing the most recent advances in technology, it should be possible (so it is easy to believe) that the light rays could be focussed onto an infinitesimally small spot. The radiation density would then be so high at that point as to raise the temperature to near infinity, certainly hotter than the surface of the sun.

Such an experiment must be impossible, as it would violate the second law of thermodynamics by allowing heat to be spontaneously transferred from one body to another at higher temperature. From an optical standpoint, the futility of the experiment lies in that the rays of the sun are not parallel, and can only be made more coherent with a concommitent decrease in light intensity. Regardless of the focussing system employed, light from the sun can only be focussed to the maximum extent where the light intensity per unit solid angle is the same as at the surface of the sun.

From a statistical standpoint, light emission from the sun, as is true of electron emission from a source of photoionization, is a random process. The point of origination of a light photon (or an electron), or the angle at which it is emitted, follows some probability function, and no focussing system, no matter how ingenious, can remove the random component limiting the quality of the beam.

The inherent limitation of the entrance electron optics to collimate the electron beam entering the analyzer is a major factor in considering the theoretical limits of energy analysis. Energy analyzer design ultimately consists of compensating for this inadequacy of the entrance optics.

The attainment of high resolution in electron spectroscopy (or for that matter, any form of spectroscopy) may be viewed as a struggle against the second law of thermodynamics. As an electron beam passes through an electron spectrometer, being generated by photoionization or thermionic emission at a cathode and then possibly undergoing scattering or exciting secondary electron emission, a net process of randomization of the electron beam occurs.

This degradation of beam quality must be accepted stoically, since any process of photoionization, thermionic emission, scattering or secondary electron ejection is subject to randomness of the direction of the resulting electron which cannot be eliminated or compensated for. Thus, the considerable loss of electron beam intensity associated with energy analysis should not be attributed directly to energy analysis itself, but rather to the randomizing process which preceded it. It is indeed possible to pass the electron beam emerging from the exit slit of

an energy analyzer through an additional energy analyzer without additional loss of beam intensity. In this way energy analyzers may be operated in tandem without loss from the beam because no randomization process occurs between each successive energy analysis. In actual practice, the operation of two energy analyzers in tandem is often desirable in order to suppress the transmission of electrons scattered from the electrodes of the initial energy analyzer (another method of preventing the transmission of electrons scattered from electrode surfaces which has recently been advanced, involves the machining of a shallow sawtooth profile into the electrode surface[16]).

III THE LIMITATIONS OF ELECTRON ENERGY ANALYSIS

The previous chapter has briefly investigated several specific types of analyzers and emphasized that certain limitations exist which prescribe the attainable resolution and transmission. A study of the available literature however tends to obscure the remarkable similarity of operation of the different types of energy analyzers. Generally, each analyzer is presented as an isolated entity, whose characteristics and merits are discussed without reference to other available energy analyzers.

Some efforts have been made to compile the characteristics of different energy analyzers[14]. Published papers which have compared the performance of analyzers[17,18,19] have limited their scope to a comparison of aberration coefficients for different configurations of energy analyzers, most notably the hemispherical and cylindrical mirror analyzer which jointly share their current position in analyzer technology as "king of the jungle".

It is the contention of the author that it would be a more profitable outlook to regard analyzers in a general way and formulate a theory of energy analysis. The exact characteristics of the electric field within the electrodes of the energy analyzer appear to be of no fundamental significance. Rather, how the electric field is utilized appears to determine the ultimate limitations of the analyzer.

The following discussion deals with such an approach in a model of a first order focussing analyzer. Second order focussing analyzers (for which $d^2s/d\theta^2 = 0$) will then be regarded separately as a modification of a first order focussing system. The theory considers the ultimate ability of an energy analyzer to achieve high resolution in analyzing a low

intensity electron beam. The assumption of a low current electron beam is justified because only in this case will the limitation of low analyzer transmission required for high resolution be of significance. Space charge effects due to the repulsion of electrons within the analyzer, consequently need not be considered.

The neglect of space charge is normally completely applicable for energy analysis. However, space charge effects may play an important role in the operation of electron monochrometers[20], which energy analyze the high current electron beam from an electron gun. Even in this case though, the conditions of optimal operation provided by the following theory are exactly those which have been shown[21] to best minimize the undesirable effects of space charge.

First Order Focussing Energy Analyzers

Consider a general attempt to design a high resolution energy analyzer. An incident electron (or ion) beam of brightness B_E (electron current of kinetic energy E/unit area, unit solid angle) impinges upon the entrance slits of the analyzer, which are set to define the area of the electron beam entering the analyzer, and the angular range which will be transmitted into the analyzer.

An electron entering at the center of the angular range accepted into the analyzer will follow a central ray trajectory so that it is focussed onto a point whose position on the image plane depends upon the kinetic energy of the electron. All electrons of the same energy should, at least to a first order approximation, be focussed onto the same small area on the image plane, regardless of the angle at which the electron enters the analyzer (see figure 6).

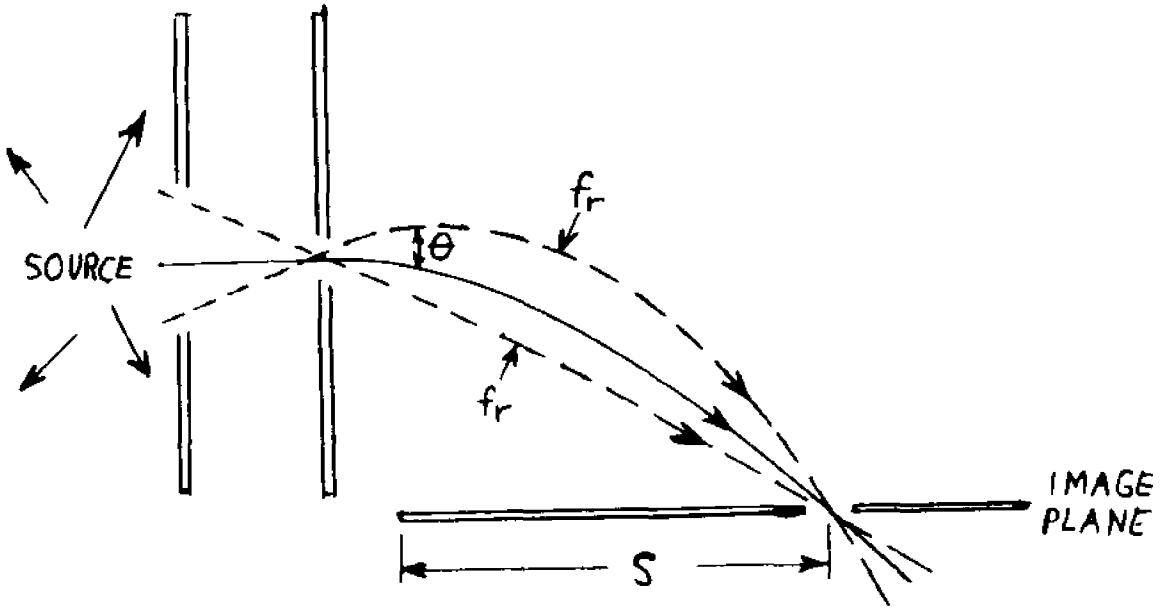

Figure 6. Diagramatic representation of the features and operation of an energy analyzer.

Another electron of the same kinetic energy originating at the same point, but with a slightly different angle of entry should also be focussed onto the same image point, although by traveling a slightly different trajectory. Such focussing can be achieved if some additional restoring force, f_r, is placed upon an electron in the alternate trajectory, in addition to the force experienced by the central ray electron. The restoring force, which is perpendicular to the alternate beam trajectory, converges the electrons toward the central ray path, eventually bringing the trajectories to cross at a focussing point.

It is clear that the restoring force must be some function of the separation from the central ray trajectory and of the distance, l, along the trajectory. For a small separation, r, from the central ray trajectory, the restoring force is described by:

$f_r = H(1)r$

where H(1) is some function varying with the coordinate of distance along the trajectory.

If H(1) is a constant value, a harmonic restoring force is present, so that the separation from the central ray trajectory varies sinusoidally with a characteristic time period. At some distance along the central ray trajectory, the paths of all electrons of the same energy will cross, independent (to a first order approximation) of the initial angle of entry θ into the analyzer.

If only first order effects were considered, utilization of this focussing property would allow ideal, aberration-free energy analysis to be achieved. The focus point would be chosen to coincide with the image plane, so that the position S at which electrons strike the image plane would depend only upon the kinetic energy of the electron. Such a naive outlook however is only acceptable when an extremely narrow angular range is accepted into the analyzer (severely restricting the number of electrons transmitted by the analyzer). An attempt to enhance the transmission of the analyzer by allowing a larger angular range of electrons to enter the analyzer will result in a second order focussing aberration, degrading the ability of the analyzer to focus electrons of identical kinetic energy to the same focus point.

Because the restoring force brings the trajectories of electrons to the focus point <u>independently of the velocity component perpendicular to the central ray trajectory</u>, an inherent aberration of the analyzer is present. The position that an electron strikes the image plane, S, will depend only upon the energy associated with the velocity component along

the central ray trajectory, $E_x = E_o \cos^2\theta$. It will then be true that:

(III-1) $$S = kE_x + S_o$$

where k is a constant depending upon the dimensions of the analyzer, and S_o is an arbitrary constant depending upon the choice of the coordinate system.

An electron of energy E entering along the central ray trajectory ($\theta = 0$) will intersect the image plane at a farther point than an electron of the same energy entering at an angle θ from the central ray. If electrons entering the analyzer are restricted to within an angular range θ_{max} from the central ray trajectory, the electrons of the same energy E will focus over a range ΔS on the image plane, where

$$\Delta S = S_{max}(\theta=0) - S_{min}(\theta=\theta_{max})$$

$$\Delta S = kE - kE\cos^2\theta_{max}$$

$$\Delta S = kE\sin^2\theta_{max}$$

For the small values of θ_{max} required for high resolution, the equation may be simplified to:

(III-2) $$\Delta S = kE\theta^2_{max}$$

An ideal energy analyzer should be capable of discriminating between electrons of nearly identical energy. However, the failure of the analyzer to focus electrons of each energy to a distinct point on the image plane will result in the overlap of trajectories of electrons of similar (but different) energies on the image plane. Electrons of different energies will be focussed to the same slit on the image plane if the energy components E_x are sufficiently similar such that the widths of the analyzer slits (s_1+s_2) is greater than the dispersion of the analyzer. An analyzer allowed to accept electrons within an angular range $\pm\theta_{max}$ from the central

ray trajectory will be marginally unable to completely resolve electrons of energy E_H and E_L under the condition:

$$S_{min}(E_H) - S_{max}(E_L) = s_1+s_2$$

$$S(E_H, \theta=\theta_{max}) - S(E_L, \theta=0) = s_1+s_2$$

Taking Eqns. (III-1) and (III-2) into account, it is seen that there exists a small range of electron kinetic energies, $\Delta E = E_H - E_L$, within which the analyzer cannot discriminate.

$$\Delta E = E\theta^2_{max} + IE \qquad \text{(III-3)}$$

where $I = (s_1+s_2)/(S-S_o)$, an analyzer constant

Commonly, electron energy analyzers are not designed with the electrons entering upon an axis of symmetry. As a result, the angular range accepted into the analyzer is rarely a conical section within an angle θ_{max} from the axis. (although this situation is attained in spherical retarding analyzers[22,23]). Instead, the analyzer is usually designed

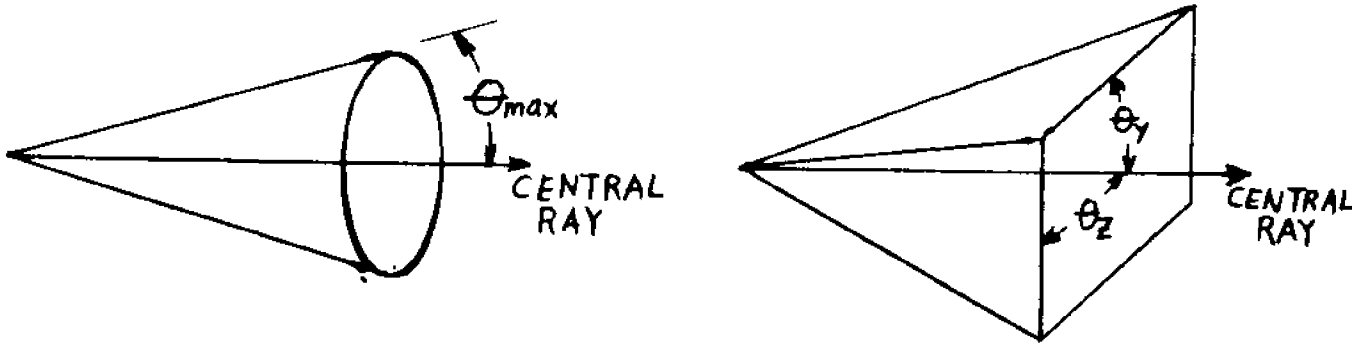

Figure 7. Angular Acceptance Ranges from a Source

to accept electrons within a rectangular pyramid acceptance range, arising from two mutually perpendicular angular ranges $\pm\theta_y$ and $\pm\theta_z$. Both angular ranges may contribute to the aberration of the analyzer, and it can be shown that in this case, that maximum resolution and transmission will simultaneously be achieved when $(\theta_y)_{max}=(\theta_Z)_{max}$. Under this optimal condition, the angular range $\pm(\theta_y)_{max}$, $\pm(\theta_z)_{max}$ constitutes a solid angle Q, given by $Q = 4\theta^2$ (where $\theta = (\theta_y)_{max} = (\theta_z)_{max}$).

Then,

(III-4) $\Delta E = EQ/2 + IE$

Thus even when no additional focussing aberrations are present, the ability of the analyzer to discriminate between electrons of slightly different energies is limited by the maximum acceptance angles of the analyzer and the energy of the beam. The energy resolution of the analyzer can be increased by minimizing the angular range accepted into the analyzer, although the transmitted current will then be decreased.

In fact, a fundamental trade-off exists between resolution and transmission, whereby one may be increased at the sacrifice of the other. Any consideration of analyzer performance must consider the resolution and transmission attained simultaneously under a giv en set of operating conditions.

If solid angular range Q is accepted from each point in the source area, then the electron current of kinetic energy E transmitted by the analyzer is given by

(III-5) $T_E = B_E A_S Q$

where B_E is the brightness of the beam at kinetic energy E, and A_s is the source area perpendicular to the central ray.

An electron beam originating at a source of brightness B_s can only be increased in brightness by acceleration of the beam to higher energy, regardless of any electron optical system employed[24,25]. Upon acceleration or deceleration of source electrons formed with energy E_s, to energy E_E at which the electrons enter the analyzer, the maximum brightness of the beam which can be attained is given by:

$$B_E = B_s(E_E/E_s) \qquad \text{(III-6)}$$

Incorporating Eq. (III-6) into Eq.(III-5) provides the current of electrons of energy E_E entering the analyzer.

$$T_E = B_s A_s Q(E_E/E_s) \qquad \text{(III-7)}$$

When combined, Eq. (III-4) and (III-7) provide a limitation on the resolution and transmission which can be achieved concurrently with a first order focussing system in the absence of symmetry focussing. For an electron source of area A_s, brightness B_s and energy E_s:

$$T_E = 2B_s A_s(\Delta E/E_s - IE_E/E_s) \qquad \text{(III-8)}$$

First Order Focussing, No Symmetry Focussing

A curious consequence of Eq. (III-8) is that the instrumental effect of the slitwidth ($I= (s_1+s_2)/S-S_o$) on the degradation of resolution and transmission may be reduced either by increasing the physical dimensions of the analyzer image plane, or by decelerating the beam to low energy before entry into the analyzer. Thus the effect of slitwidths is not an inherent limitation on the ultimate resolution and transmission which may be obtained simultaneously. Consequently, some improvement in performance will generally be achieved by deceleration of the beam before entrance into the analyzer. The improvement attained however will be limited, and even if the degrading effect of slit widths is completely nullified, the ultimate

performance attainable with such a first order focussing analyzer is given by,

$$(III\text{-}9) \qquad T_E = 2B_s A_s \, \Delta E/E_s$$

The energy with which electrons are ejected from the source plays a critical role in determining the attainable performance of the analyzer. If, for example, electrons are to be collected within a 30 meV "energy window", those electrons ejected from the source at an energy of about 10 eV could be transmitted through the analyzer ten times more efficiently than electrons released with 100 eV. Of all electrons ejected from the source within a complete spherical 4π stearadian solid angle, the fraction of electrons formed with energy E_s transmitted by the energy analyzer is readily shown to be:

$$(III\text{-}10) \qquad \text{fraction electrons transmitted} = (1/2\pi) \, (\Delta E/Es)$$

As an illustration, if source electrons of 10 eV kinetic energy were to undergo ideal first order energy analysis (without symmetry focussing) so that only electrons within a 30 meV energy window were transmitted, then only about one electron in 2,000 with 10 eV energy would be transmitted. Electrons of kinetic energy outside the energy window, of course, would not be transmitted, and the overall collection efficiency for electrons of all energies is quite low, typically of the order of 10^{-6}.

A direct implication of this line of reasoning is that very low energy electrons could conceivably be energy analyzed with collection efficiencies (for electrons within the energy window) approaching unity. Although the author initially regarded this as merely a theoretical possibility, a low energy "stearadiency analyzer" has been developed[26]

collects virtually all incident electrons of low energy, resolving 30 meV energies. Furthermore, the mechanical construction of such analyzers is remarkably simple.

The reader may at this point question the significance of the energy at which the electrons are produced in the source. Electrons, it may be argued, can readily be decelerated to low energy, so cannot high energy electrons be decelerated and disquised as low energy source electrons?

Despite cleverness and deception on the part of the cunning experimenter, this cannot occur. Upon deceleration of the source electrons to low energy, the brightness of the beam is unavoidably decreased, and the transmission suffers proportionately. Regardless of the type of energy analyzer employed, electrons formed in the source at low energy are intrinsically easier to energy analyze than high energy electrons.

It is clear then that a source of low energy should be employed where possible. In the case of photoelectron spectroscopy, radiation as near to the ionization threshold as possible should be used, provided that a high cross-section for photoionization is maintained. For example He(I) radiation (of photon energy 21.2 eV) inherently provides superior transmission and resolution than He(II) radiation (of 40.8 eV energy) for orbitals of sufficiently low ionization potentials, from a factor of about two (at near zero IP's) to nearly unlimited improvement (at IP's near 21.2 eV).

Although Eq. (III-9) represents the performance which may be achieved with a first order focussing analyzer without symmetry focussing, it is possible to incorporate certain focussing properties which could allow a

substantial improvement in the capability of the analyzer. Nonetheless, it will become apparent that all energy analyzers may be considered simply as modifications of this basic scheme.

Before proceeding to consider analyzers with additional focussing properties, it is useful to consider how the capability of first order non-symmetry focussing analyzers may best be realized. Although the fraction of electrons within the energy window transmitted by this type of analyzer is relatively low, the use of a large source area allows large numbers of source electrons to be formed, and consequently, a large electron current to be transmitted by the analyzer. The use of large source areas tends to aggravate the degradation of resolution due to the slitwidth, although this may be overcome by decelerating the beam before entry into the analyzer (as suggested by Helmer and Weichert[27]), or by the use of energy compensation (as done by Marmet[28]). By using the energy compensation technique, Marmet has designed and constructed analyzers with very large source areas (4X6 mm), yet maintaining a 40 meV wide energy window.

Energy compensation involves the presence of an electric field, F_y, within the source region so that electrons originating at a point $y=y_o$ will have acquired an additional energy increment, $F_y e y_o$, before entering the analyzer. The point of entry of an electron into the analyzer is therefore correlated with the additional energy component acquired. Consequently, the analyzer can be designed to focus each area element of the source onto a narrow slit on the image plane by compensating for the position on the source area with the additional energy increment gained by the electron.

The energy increment acquired is small compared to the kinetic energy

of the electron, so that the effect of the field F_y may be considered as a small perturbation not seriously affecting the trajectory of the electron before entry into the analyzer. Guard electrodes within the analyzer are required to insure that only electrons within a small angular range from each point in the source are transmitted by the analyzer.

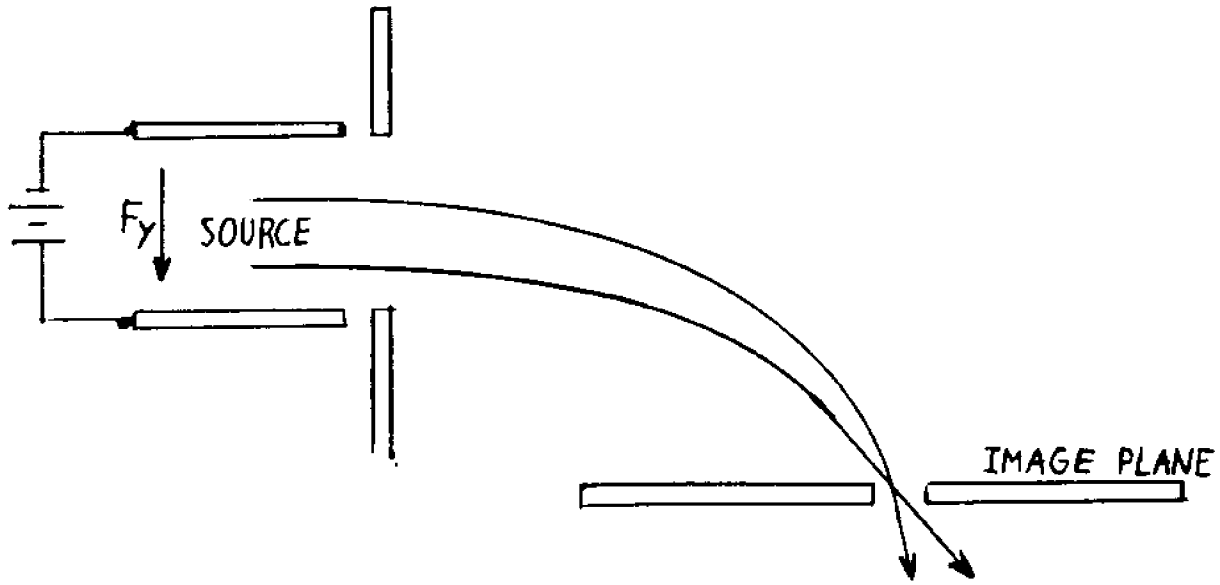

Figure 8. The Use of Energy Compensation to Focus Each Area Element of a Large Source onto the Image.

Another means of applying energy compensation, particularly in photoelectron spectroscopy, is by the use of "dispersion compensation"[29,30]. In this technique, x-ray radiation from a continuous source is dispersed by a diffraction grating so that the energy of the radiation varies over the irradiated source area. The kinetic energy of the resulting photoelectrons will therefore be correlated directly with the position of the point of origination in the source. Introduction of an additional focussing property allows each element of the correlated source area to be focussed onto a narrow slit in the image plane.

The similarity of energy compensation techniques and another compensation technique, subsequently to be called second order focussing, will later become apparent.

Symmetry Focussing

In the preceding mathematical analysis, both of the two mutually perpendicular angles characterizing the trajectory of an incident electron were presumed to contribute to the aberration of the analyzer. However, this need not be the case. Since dispersion of the electrons according to their energy need only occur along one coordinate, the angular spread of the beam in the perpendicular direction need not necessarily have any degrading effect on the attainable resolution.

To illustrate the point, once again it is possible to utilize the simplicity of the parallel plate analyzer. Recall that within the constant electric field between two parallel plates, the electron paths are the same parabolic trajectories followed by a cannonball subject to the force of gravity.

Envision, if you will, a cannon situated in the center of an enormous flat field. The cannon is mounted so that the direction of fire can be varied by changing the angle of elevation, or by rotating along the lateral angle (these are two mutually perpendicular angles which can be independently varied).

At this point, cannonballs of the same energy can be fired and the position of impact upon the field (image plane) observed. It will be found of course that at an angle of 45° the cannon will have the maximum range and that, to a first order approximation, the distance traveled by

the projectile will be independent of the elevation angle near 45^{o}. An aberration will result however due to the range of elevation angles centered about the central ray trajectory at 45^{o}, and as a consequence, the cannonballs will not all land at precisely the same distance S from the cannon. Rather, the projectiles strike the field over a range ΔS.

Apparently then, a focussing aberration is present associated with the range of angular elevation, resulting in an inability to resolve completely the trajectories of projectiles of slightly different energies.

Now however, the gun crew is instructed to permanently set the angle of elevation of the cannon to 45^{o}, and the cannon is rotated in the lateral direction. As the cannon is repetitively fired, it will be observed that the projectiles strike the field along the arc of a circle, whose center lies at the position of the cannon. It is now attempted to fire the cannonballs into a straight ditch (slit) tangent to the radius of the circle. It will be observed that at one lateral angle (such that the cannonball trajectory is perpendicular to the ditch), the cannonball lands directly in the ditch. Should the cannon be rotated in either direction by a small lateral angle though, the projectile falls short of the ditch. Consequently, a focussing aberration is then associated with the lateral angle of the cannon: a cannonball of slightly higher energy will land in the same ditch if it is fired at some lateral angle from the central ray trajectory.

Indeed, in considering these hypothetical experiments, the reader has just witnessed the operation of a non-symmetry focussing configuration of the parallel plate analyzer. Both the lateral and elevation angle of an incident particle have contributed to the aberration of the analyzer.

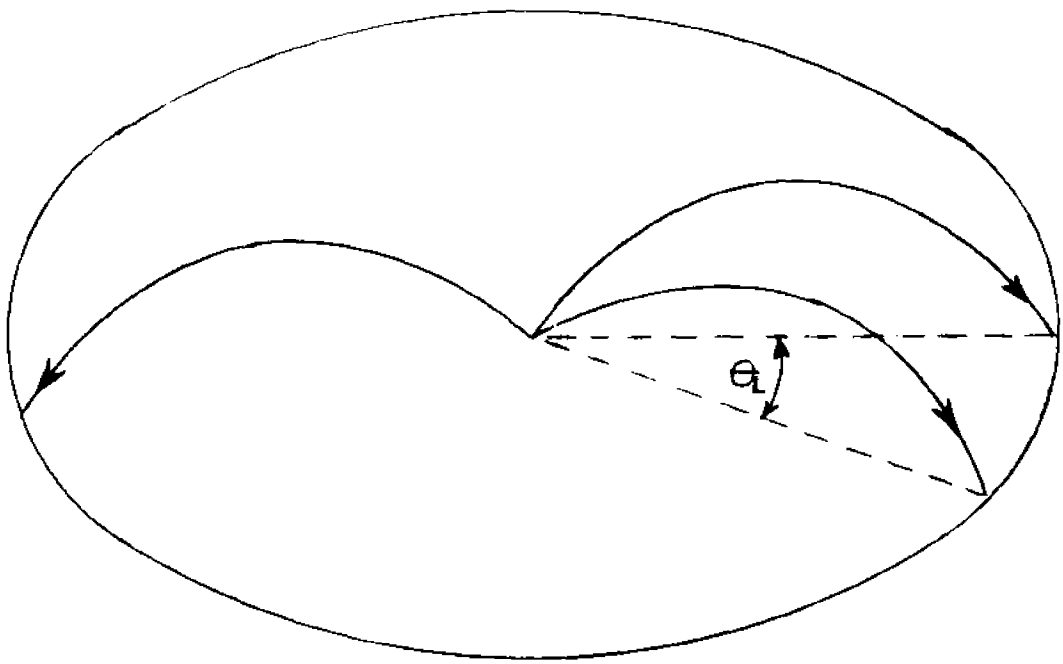

Figure 9. Variation of projectile trajectory with lateral angle θ_L

A much higher efficency of collection of the projectiles could be realized however if, rather than using a straight ditch, a circular ditch were employed which entirely encircled the cannon. Then, the lateral angle at which the cannonball is fired would result in no focussing aberration whatsoev er. All projectiles within an entire 360^{o} lateral angle could then be collected without any degradation of the attained resolution. Obviously, a configuration of such symmetry would allow much higher numbers of cannonballs (or electrons) to be collected, while maintaining the same resolution.

In a direct application of these principles to electron energy analyzers (demand for cannonball analyzers has been slack), far superior performance could be attained, at least in theory, by the use of a "fountain-type" parallel plate analyzer whereby electrons are accepted over an entire 360^{o} range of lateral angles and transmitted through a circular slit.

The "fountain-type" parallel plate analyzer has not found widespread application due to the extensive region through which electrons exit the large circular slit. Collecting these electrons for entry into an electron multiplier or an electron optical system would prove in reality to be ungainly and impractical.

A much more elegant manner of providing such symmetry focussing is provided by the hemispherical analyzer, where the symmetry of the two concentric spherical electrodes is utilized. Electrons entering the analyzer with various "lateral" angles θ_z travel in great circle trajectories along a spherical surface and emerge from a small exit slit. Only the perpendicular angular range θ_y will degrade the resolution of the analyzer.

An expression analogous to Eq. (III-8) may be derived for the limitation of transmission with a given resolution, where symmetry focussing is present. Eqn. (III-6) relating the increase in brightness with energy is no longer directly of interest. Acceleration of an electron beam to a higher energy E_E will compress the angular divergence so that a greater current will be within the angular range $\pm\theta_y$, $\pm\theta_z$. However, when symmetry focussing is present, compression of the angular divergence $\pm\theta_z$ results in no increase in transmission since the analyzer is capable of transmitting electrons with any angle θ_z. Only the increase in brightness with respect to the angular range $\pm\theta_y$ is of interest, given by:

(III-6B) $$B_E = B_s(E_E/E_s)^{\frac{1}{2}}$$

The angular range accepted into the analyzer $\pm\theta_y$, $\theta_z = \pm\pi$ constitutes a solid angle $4\pi\theta_y$, so from Eqns. (III-5) and (III-6B)

(III-7B) $$T_E = B_s(E_E/E_s)^{\frac{1}{2}}A_sQ$$

Incorporating Eq. (III-3),

(III-8B) $$T_E = 4\pi B_sA_s(\Delta E/E_s - IE_E/E_s)^{\frac{1}{2}}$$

360° Symmetry Focussing, First Order Focussing

Comparing Eqns. (III-8) and (III-8B), it is seen that symmetry focussing, if fully exploited, allows a considerable improvement in transmitted current at a given resolution. Maximum benefit of symmetry focussing is derived at high resolution, the condition where the need for high transmission is most critical.

Once again, the effect of slitwidth on the degradation of analyzer performance may be reduced by increasing the physical dimensions of the analyzer, decelerating the beam to low energy before entry into the analyzer, or by the use of energy compensation. If the effect of slitwidth is

entirely eliminated, th en the ultimate performance attainable by first order focussing analyzers is given by:

(III-9A)	$T_E = 2B_s A_s \Delta E/E_s$	No symmetry Focussing
(III-9B)	$T_E = 4\pi B_s A_s (\Delta E/E_s)^{\frac{1}{2}}$	Maximum Symmetry Focussing

At a typical overall resolution, $R = E_s/\Delta E$ of 300, maximum utilization of symmetry focussing allows an improvement in the transmission by a factor of about 100. Practical design difficulties however usually prevent the full benefit of symmetry focussing from being realized.

SECOND ORDER ENERGY ANALYSIS

Equations (III-9A,B) set an upper limit of attainable resolution and transmission when electrons from a source are focussed directly onto an image. This limitation stems from the inherent aberration of the analyzer resulting from the angular range accepted into the analyzer. If the same electron current could be compressed into a beam of narrower angular divergence, it would be possible to achieve higher resolution while maintaining the same transmitted current.

An increase in the electron current per unit solid angle could be achieved in two ways. An increase in the beam energy will increase the brightness of the beam, although this will prove to be of no benefit (in fact, it has been shown that deceleration of the beam before entry into the analyzer is desirable). Alternately, the area of the beam may be increased, leading to a higher current per unit solid angular range, although the brightness of the beam remains the same.

Consider an electron beam eminating from a source (of area A_s) with

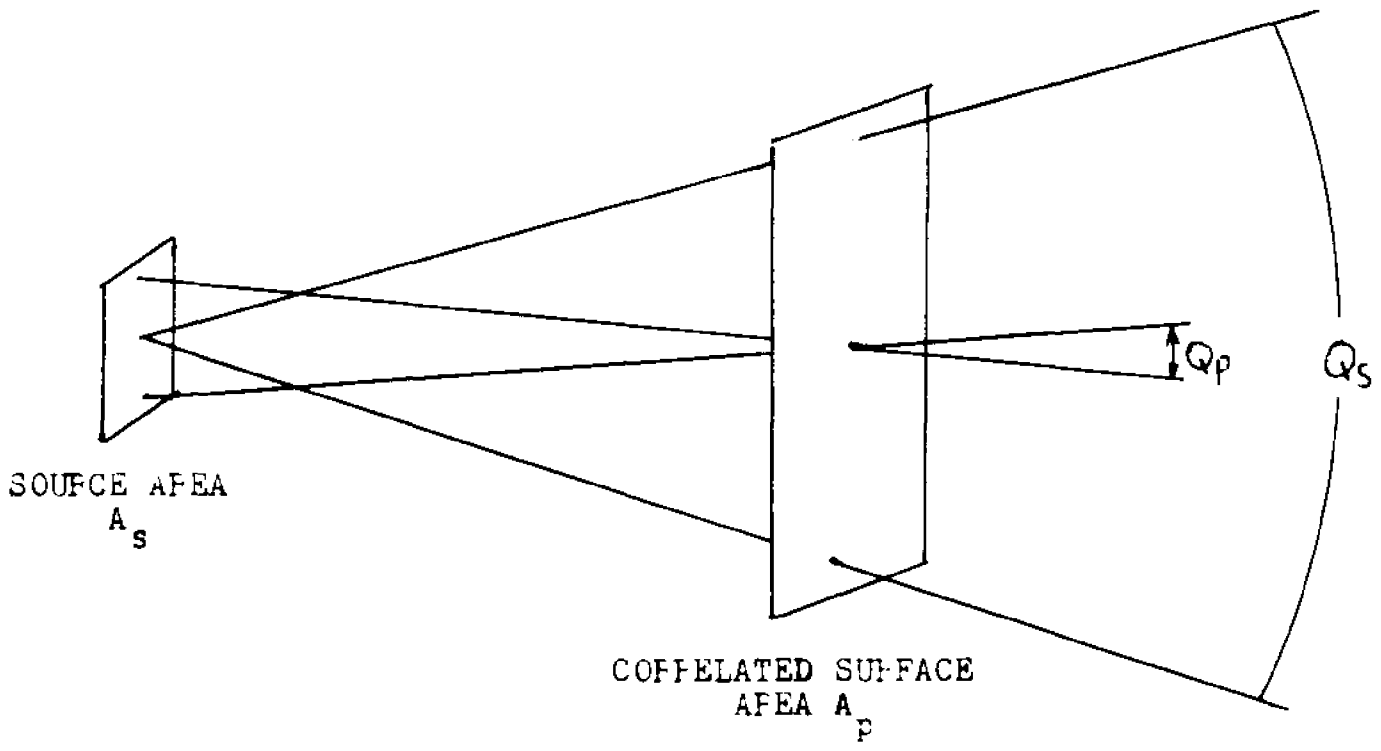

Figure (10)

Although the electron beam passing through surface P has a solid angle Q_s, a smaller angular range Q_p is present at each point in the surface. The angle of the central ray within Q_p is correlated with the position on surface P.

angular range Q_s. Should the beam be allowed to travel out in free space and expand to a larger area A_p, the beam of course will still occupy a total angular range Q_s. However, the angular range at each point in the beam will then be much less (see fig.(10)). Each area element of the expanded beam may then be focussed onto an image with a reduced aberration.

In order to transmit the entire current of electrons eminating from the source, it will be necessary to focus each area element of the expanded beam area A_p onto the image. This may be accomplished if another focussing property (very similar to energy compensation) is introduced so that electrons (of the same energy) from each area element of the expanded source area A_p are focussed onto the same image.

Referring to fig.(10), note that by projecting (or focussing) the electron beam onto a surface of large area A_p, while the angular range at each point in the expanded beam is relatively small, the angle of the central ray at each point on surface P is correlated with the position on the surface. The analyzer will then be able to focus each area element of surface P onto the image by compensating for the position of the area element with the central angle of the beam at that point.

The utilization of such a second order focussing property allows a substantial improvement in resolution (or alternately, higher transmission at the same resolution) depending upon the extent that the beam is expanded in area before being focussed onto the image.

Another way of viewing second order focussing is by considering an analyzer which simultaneously accepts several small angular ranges through

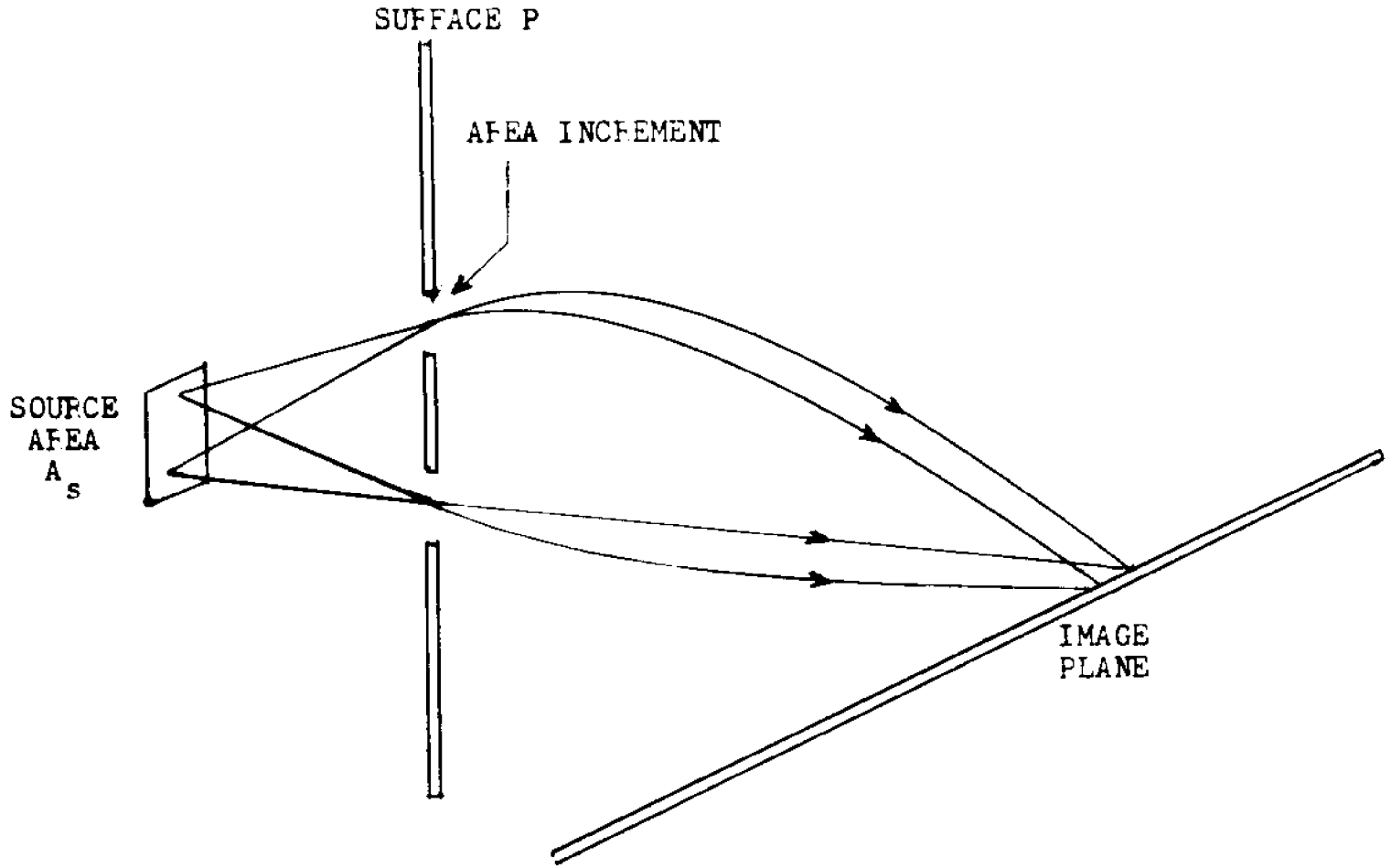

Figure(11)

An analyzer employing second order focussing to independently focus several pencils of electrons onto the image.

a series of (imaginary) slits. (see fig. (11)). Each pencil of electrons accepted through a slit is focussed onto the image plane, and an additional focussing property allows each slit to be focussed onto the same image. The transmission of the analyzer will then be enhanced by a factor of the ratio of the total slit area A_p (which is focussed onto the image) to the source area A_s. Consequently, the second order of focussing improves the performance of the analyzer by a factor of (A_p/A_s), where A_p is the maximum area focussed onto the image, in which the angle of entry is correlated with the position on the surface[15].

The current of electrons of energy E transmitted by the analyzer when second order focussing is incorporated, is given by:

(III-11A) $$T_E = 2B_s A_p (\Delta E/E_s - IE_p/E_s)$$ no symmetry focussing

(III-11B) $$T_E = 4\pi B_s A_p (\Delta E/E_s - IE_p/E_s)^{\frac{1}{2}}$$ complete symmetry focussing

where E_p is the kinetic energy of the expanded beam entering the analyzer.

Although this treatment does not constitute a rigorous proof, it appears that Eqns. (III-11A,B) in fact represent the fundamental capabilities of energy analysis employing a single channel of detection. Optimal conditions have been assumed in this derivation, and when effects of lens aberrations and distortions, surface charging, and incomplete utilization of symmetry focussing are considered, actual performance will inevitably be inferior to that predicted here.

The geometry of the cylindrical mirror analyzer has proven to be particularly suitable for providing second order focussing, as well as a large degree of symmetry focussing. Note that the term "second order

focussing" should be interpreted primarily as a mathematical concept, rather than a physical entity. Depending upon how the electric field is utilized, the cylindrical mirror analyzer may be operated with first order focussing in the slot-to-slot mode[11], or as second order focussing in the point-to-point mode[10].

An intriguing implication of Eq. (III-11A,B) is that second order focussing analyzers are not subject to any inherent absolute limitation upon the attainable transmission at high resolution. Presumably, projection of the incident electron beam upon an immense correlated area, which is focussed onto the image, would allow virtually all electrons within the energy window of the analyzer to be collected (of course, with a single channel detection system, electrons outside the energy window would be rejected by the analyzer). The analyzer which probably has the potential of most closely approaching this ideal situation is the combinatination spherical retarding-spherical reflecting analyzer described by Lee[23]. The ability of this analyzer to transmit a large fraction of the source electrons is theoretically limited only by the physical dimensions of the analyzer (relative to the dimensions of the source area). Although the electrode grids required to transmit the beam within the analyzer introduce the possibility of scattering or charging effects which may degrade the analyzer resolution, the spherical retarding-spherical reflecting analyzer has been incorporated into a commercially available x-ray photoelectron spectrometer built by Dupont Instruments[31]. This design strategy contrasts with the efforts of most other commercial instrument manufacturers, who have adopted configurations of hemispherical or cylindrical mirror analyzers, and have concentrated upon sophisticated multichannel detection systems to increase the rate of data collection.

Multichannel Detection Systems

Up to this point, it has been presupposed that the analyzer image plane contains one slit to transmit electrons within one small energy range ΔE. Electrons outside of this energy window are not transmitted by the analyzer. To obtain a spectrum of electron energies over an energy range $E_1 \rightarrow E_2$, it is required to scan the kinetic energy transmitted by the analyzer from E_1 to E_2, progressively collecting electrons of various energies as the energy window is shifted. Such a single channel detection system inherently has a poor collection efficiency for analyzing electrons over a broad energy range. Even if the analyzer has a high transmission for those electrons within the energy window, all those electrons of other energies will be rejected.

A logical method of improving the data collection rate is to have two, or several, slits on the image plane so that electrons of different energies will be transmitted through their respective slits and enter independent detectors. In this way, the count rate of electrons at several different energies can simultaneously be monitored. The rate of data collection can be proportionately increased through the use of additional independent detection channels (requiring an electronic multichannel analyzer to process and store the count rates provided by each detector). A limit exists however, to the number of independent detection channels which may be gainfully employed. If the analyzer is operated with an energy window ΔE, then more than one channel of detection for energy range ΔE will result in redundancy of information. Optimal multichannel analysis therefore requires one channel for each energy range ΔE over the energy range $E_1 \rightarrow E_2$ which is of interest.

In order to maintain a constant collection efficiency at all electron energies, analyzers are generally operated in the "constant resolution mode", such that the resolution R obtained, which is defined as

$$R = E_s / \Delta E ,$$

is a constant for all electron energies (this follows as a consequence of Eq. (III-10)). As a result, electrons of higher kinetic energies are analyzed through a wider energy window. Since the width of the energy window varies linearly with the kinetic energies analyzed, fewer channels are required at higher energy in order to avoid redudancy of information. It may be shown that the optimal number of channels necessary to collect electrons within the energy range $E_1 \rightarrow E_2$ with resolution R is:

for $E_1 >> 0$
when N is large $\qquad N = R \ln(E_2/E_1)$

At very low energies, practical considerations prevent the width of the energy window from decreasing below a value of ΔE_{min}, and for the energy range $E=0 \rightarrow E_2$, the optimal number of channels required is:

$$N = R \left[\left(\ln \frac{E_2}{R \Delta E_{min}} \right) + 1 \right]$$

Perhaps, it may not be desired to operate the analyzer in the "constant resolution mode", but rather to maintain the same energy window at all kinetic energies. Clearly for most purposes, a "constant window mode" is more satisfactory for the collection of electron kinetic energy spectra, and some workers in the field have chosen operating parameters so as to achieve this condition. However, what is seldom appreciated, is that operation in the "constant window mode" results in decreased collection efficiency at higher energies. From Eq. (III-10), it is apparent that the fraction of electrons collected within a window of constant width is

inversely proportional to the electron energy. The rate of data collection in each channel is no longer constant, but becomes progressively less for those channels of higher energy. The number of channels necessary for the energy range $E_1 \rightarrow E_2$, operating in the "constant window mode" is simply:

$$N = (E_2 - E_1)/ \Delta E$$

Regardless of whether the "constant resolution" or "constant window" mode is utilized, the total rate of data collection in all channels will be essentially the same.

Energy Analysis Systems

The electrode geometry of an energy analyzer in itself provides a poor basis for the evaluation of its possible performance. Rather, the configuration of the preceding slits and electron optics, and how the electron field is utilized are primary considerations which must be taken into account. These determine whether the analyzer provides symmetry focussing, second order focussing, can accommodate a large source area or allows multichannel detection systems. A dogmatic statement for example, that the spherical electric field of the hemispherical analyzer allows high resolution and transmission to be achieved , neglects the way in which the field is utilized. Various configurations of the hemispherical analyzer have been proposed[9,32], varying in the ability to accommodate large source areas, and may vary in the utilization of symmetry focussing.

In order to anticipate the properties and limitations of energy analysis and how these may best be achieved, it is necessary to think in terms of the entire energy analysis system. Two basic systems may be envisioned, shown in Fig. (12A,B), to provide either "constant window" or "constant resolution" operation. In essence, the system consists of

Fig.(12) A. Operation of an Energy Analyzer in the "Constant Window" Mode

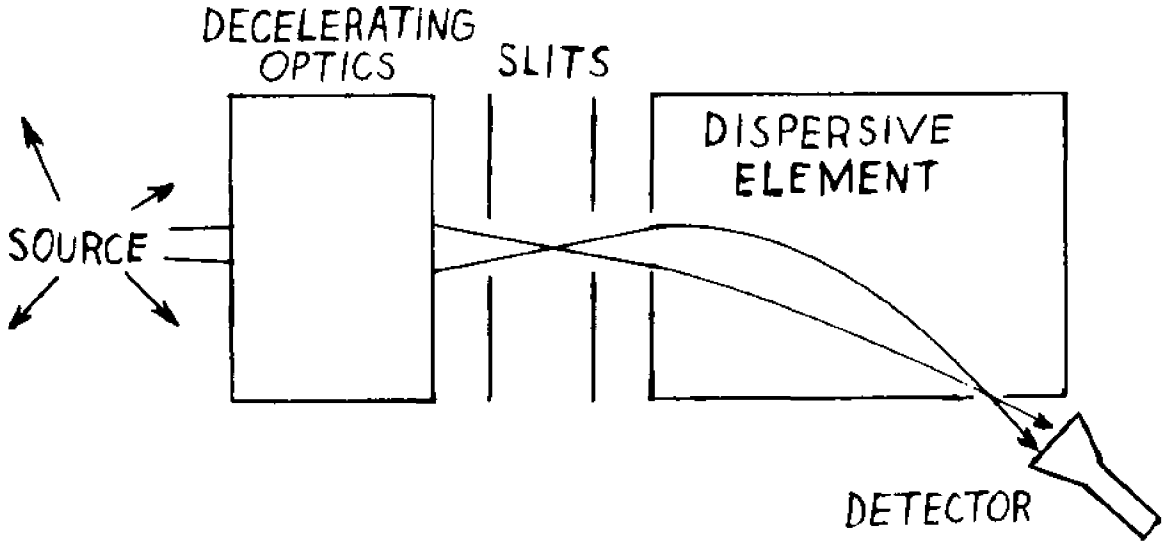

B. Operation of an Energy Analyzer in the "Constant Resolution" Mode

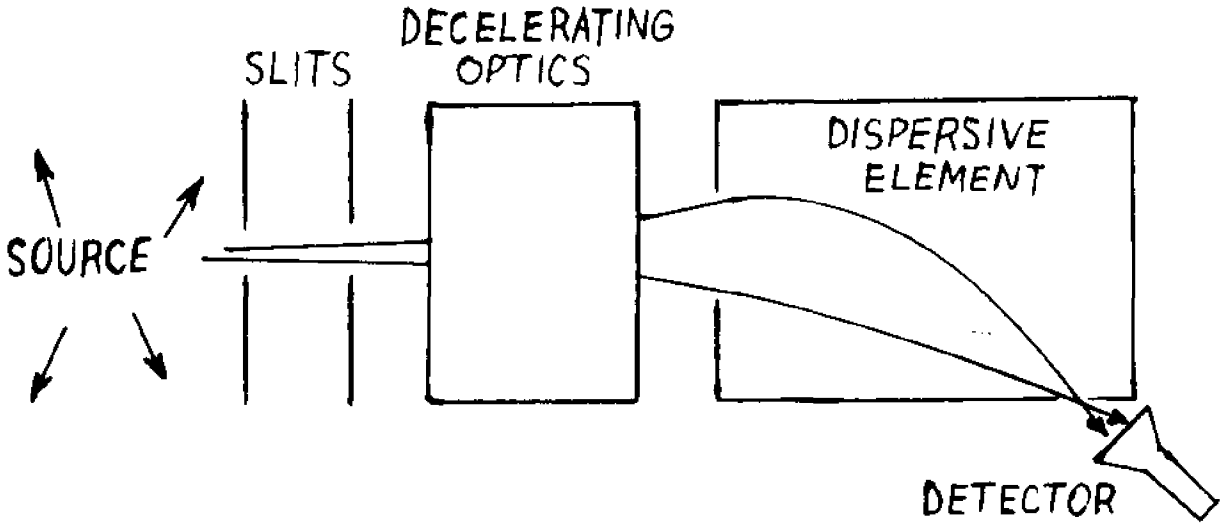

several basic components. A system of decelerating electron optics decreases the energy of the electrons from their energy in the source E_s to the energy at which they are admitted into the analyzer, E_E. A series of properly located slits then limits the transmitted electrons to those within a specified angular range (the higher the resolution required, the smaller must be the angular range accepted). The dispersive element (commonly referred to as the analyzer itself) disperses the electrons according to their kinetic energy, and then the detection system collects electrons of predetermined energy (or energies).

In the "constant window" mode, shown in Fig. (12A), electrons from the source within the energy range to be transmitted, are decelerated to an energy at which they enter the analyzer, E_E, which always remains constant. As the angular range allowed to enter the analyzer remains predetermined by the slit system, the analyzer resolution $R_A = E_E/\Delta E$ remains constant, resulting in an energy window of constant width, ΔE, regardless of the energy at which the electrons are formed in the source. The system resolution, $R_S = E_s/\Delta E$, increases at higher source energies due to the constant width of the energy window. The fraction of source electrons transmitted by the analyzer decreases as the source energy is increased. This is due to the greater deceleration that the higher energy source electrons undergo (so that their brightness at the slit system is decreased). As a result, fewer of the decelerated electrons are within the proper angular range to be accepted through the slit system.

Fig. (12B) shows the "constant resolution" mode of operation, in which a slit system initially accepts electrons within the proper angular range, which then are decelerated to an energy E_E and enter the dispersive

element. Since, in this case, deceleration of the electrons occurs after the slits reject those electrons outside the predetermined angular range, the fraction of source electrons transmitted is independent of the energy of the electrons in the source. Source electrons of higher energy will however occupy an expanded angular range upon entry into the analyzer (due to the decreased brightness of the beam upon deceleration) thereby resulting in a broadened energy window. A constant overall system resolution, $R_S = E_s / \Delta E$, is consequently maintained.

IV. ELECTRON LENSES

The design of energy analysis systems often requires the use of electron optical lenses. By the use of such lenses, a source of electrons may be focussed onto a magnified or demagnified image, exactly analogous to the operation of light optical systems.

Although the focussing properties of common electron lenses have been mathematically and empirically derived in standard electron optical texts[33-41], it is not presented on an intuitive basis exactly why electrons lenses actually should work at all. In the hope of meeting this objective, this chapter provides a somewhat simplified account of the operation of electron lenses.

The focussing of electrons in electrical (or magnetic) fields, electron optics, is highly analogous to light optics, whereby a light beam is focussed upon passing between media of different indices of refraction. Focussing of a light beam generally occurs only at the interface between two media, the index of refraction changing abruptly over a virtually infinitesimal distance. On the other hand, electron-optical focussing occurs over a finite (and sometimes extensive) region of space in which the potential is varying. Note that the term "potential" in electron optics (contrary to the usual notation in physics) refers to the kinetic energy of an electron at a given point in space.

Consider the action of a general electrostatic lens consisting of electrodes creating some variation of potential within a region of space (depicted in Fig. (13)). Cylindrical symmetry is commonly employed within the electrodes so that an electron traveling along the axis of the

lens will not undergo deflection within the focussing region. It is convenient to consider the focussing on an electron traveling parallel to, and near, the axis of the lens, a so-called par-axial electron. A properly designed electron lens will bring all par-axial electrons to a focus point on the axis, regardless of the initial distance of the electron trajectory from the axis.

Figure(13)

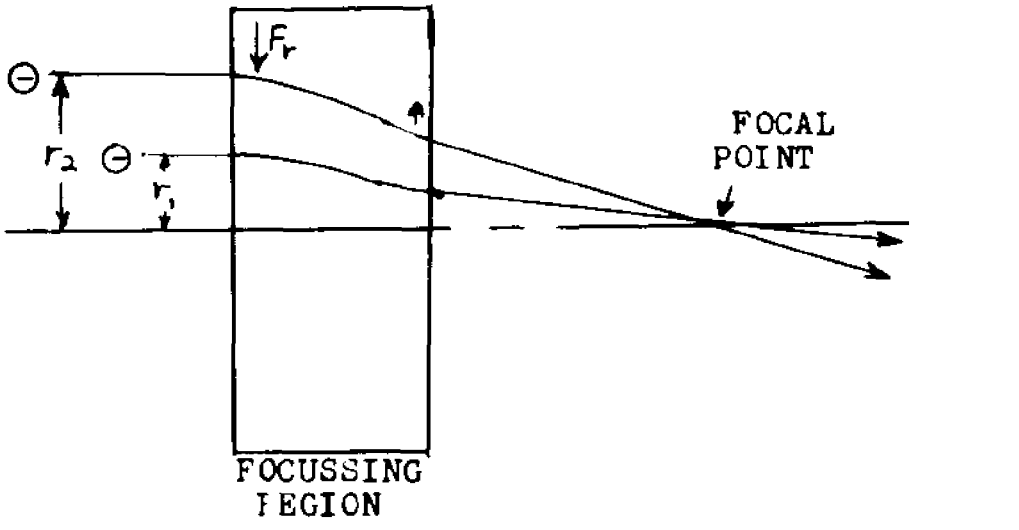

In order for electrons to converge toward the axis, some force F_r must be exerted on the electron while in the focussing region, imparting to the electron a net radial velocity v_r toward the axis. The electric field within some segments of the focussing region will converge the beam toward the axis, while other segments will have a diverging effect. The overall focussing property of an electrostatic lens however will always be converging, although this is a second order effect resulting from the difference between converging and diverging fields.

The Aperture Lens

Probably the simplest electron lens to describe is the aperture lens, depicted in Fig. (14). Electrons originating within a field-free region, held at potential V_1 by the surrounding electrode, pass through a set of apertures into a similar region at potential V_2.

Fig. (14) Cross Section of an aperture lens

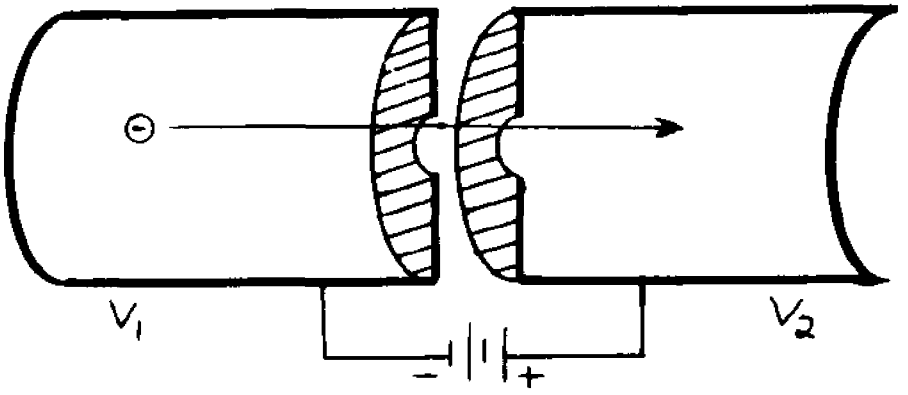

The most significant and obvious consequence of an electron passing through the region between the apertures in the two electrodes will be an acceleration to higher kinetic energy. In addition, a more subtle effect will arise due to the variation in potential near the apertures, imparting a radial velocity component to the electron. At the region near the first aperture, a radial force accelerates the electron toward the axis of the lens, while the second aperture will tend to diverge the beam away from the axis. The cummulative effect of all radial forces will be focus an electron toward the axis.

If the potential difference experienced by the electron in crossing between the two electrodes is small compared to the kinetic energy of the incident electron, then the focussing effect will be weak and may be considered as a small perturbation to the electron trajectory. This is the case most readily subject to mathematical analysis and which will consequently be considered here. A lens whose focussing is sufficiently weak that the focal length of the lens is much longer than the focussing region of the lens, is known as a "thin lens", a term originating from the analogous situation in light optics. Furthermore, the analysis of an aperture lens is greatly simplified if the assumption is made that the apertures are very small. Although it may be argued that actual electron lenses rarely satisfy the criteria of being thin lenses, or having small apertures, such a model of electron lens operation is nonetheless quite useful, as it allows at least a semiquantitative understanding of the basic operation of electron optical lenses.

In order to understand the focussing action of a thin aperture lens, let us examine the effect of the electric field near the first aperture. The electric field distortion due to the aperture may be considered as being localized with in the immediate vicinity of the aperture (within one aperture diameter). Hence, except within the immediately adjacent area, the effect of the aperture may be ignored. Within most of the region between the two electrodes, the electric field may then simply be considered as a constant field E_a in the axial direction resulting from the difference in potential (V_2-V_1) between the two parallel disc-like electrode surfaces. Furthermore, the electric field distortion due to the aperture will not penetrate more than one aperture diameter into the field-free region, so that no electric field is experienced by an incident

electron until within the immediate proximity of the aperture.

The readers attention is now directed toward the region of space near the first aperture, where the electric field distribution may be inferred from the application of Gauss's Law. This law of electrostatics states that within any arbitrary region of space, the sum of all electric field flux leaving the region is proportional to the charge contained within that region.

$$(IV\text{-}1) \qquad \sum_{\substack{\text{entire} \\ \text{surface of region}}} E \Delta A = Q/e_o$$

where ΔA is a small area on the surface bounding the region under consideration.

E is the electric field component perpendicular to the boundary surface.

Q is the total charge contained within the region.

e_o is a constant.

Gauss's Law may be applied to an imaginary cylindrical region within the aperture (concentric with the axis of the lens) of radius r and several aperture diameters long. No charge is contained within this region (except for the electrons passing through the aperture, whose space charge can be neglected for low current beams) and so, the electric field divergence leaving the region must be zero. Consequently, the electric field flux leaving the end of the cylindrical region is equal to the total radial field flux entering the sides of the imaginary cylinder.

Figure(15)

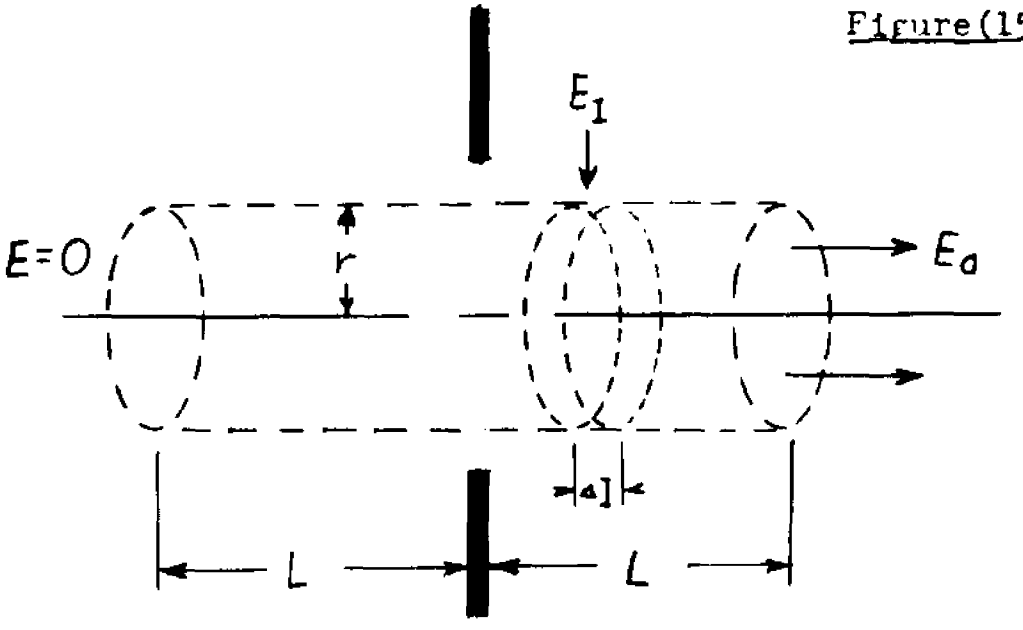

Let E_1 be the electric field perpendicular to the side of the cylinder at distance 1 from the plane electrode in which the aperture is located. Then,

$$E_a(\pi r^2) = \sum_{1=L}^{L} E_1(2\pi r \Delta 1)$$

or more exactly,

$$E_a(\pi r^2) = \int_{-L}^{L} E_1(2\pi r)d1$$

Canceling terms;

$$(IV\text{-}2) \qquad \tfrac{1}{2}E_a r = \int_{-L}^{L} E_1 d1$$

Now suppose, if you will, that an electron is initially traveling within the field-free region with kinetic energy V_1, parallel to the axis at radius r, unaware of its imminent entry into the focussing region. Upon entering the region of the first aperture, the electron experiences the radial field E_1 accelerating the electron toward the axis. However,

since the effect of the aperture is localized to within the immediate vicinity of the orifice, the electron velocity along the axis, v_1, will to a good approximation remain constant as it passes through the first aperture region. In traveling distance Δl, the electron is exposed to force E_l for a time duration of $(\Delta l/v_1)$, resulting in a change in momentum in the radial direction equal to the impulse applied.

$$m_e \Delta v_r = E_l \, (\Delta l/v_1)$$

where Δv_r is the velocity in the radial direction imparted to the electron.

The total radial velocity imparted to the electron in crossing through the first aperture region is:

$$v_r = \sum_{l=-L}^{L} v_r = \int_{-L}^{L} dv_r$$

$$v_r = (1/m_e v) \int_{-L}^{L} E_l \, dl$$

Substituting Eq. (IV-2)

$$v_r = (E_a/2m_e v_1) r \qquad \text{(IV-3)}$$

As the electron leaves the first aperture region, it is accelerated to kinetic energy V_2 by the electric field between the electrodes and arriv es at the second aperture, whose focussing effect will be diverging, i.e., imparting a radial velocity away from the axis. However, the diverging effect of the second aperture must be less than the converging effect of the first aperture for two reasons:

(1) The electron passes through the second aperture at higher velocity, transversing the region in a shorter time, and consequently experiences a smaller impulse.

(2) The electron will have been impelled to a smaller radial distance from the axis due to the focussing at the first aperture.

By identical reasoning applied to calculate the focussing effect of the first aperture, the focussing of the second aperture can readily be determined. If it is assumed that the radius of the electron does not change upon reaching the second aperture (which simplifies the ensueing analysis, although leading to an underestimation of the focussing effect of the lens), the radial velocity imparted by the second aperture will be:

$$v_r = -(E_a/2m_e v_2)r$$

where v_2 is the axial velocity of the electron upon reaching the second aperture.

The total radial velocity toward the axis imparted to the electron in crossing the focussing region of the lens is

$$v_r = (E_a/2m_e v_1)r - (E_a/2m_e v_2)r$$

$$v_r = (E_a/2m_e)\ (v_2 - v_1/v_1 v_2)r \qquad \text{(IV-4)}$$

It is now possible to demonstrate that all par-axial electrons will be focussed so as to cross the lens axis at a focus point located z distance from the center of the lens.

Fig. (16)

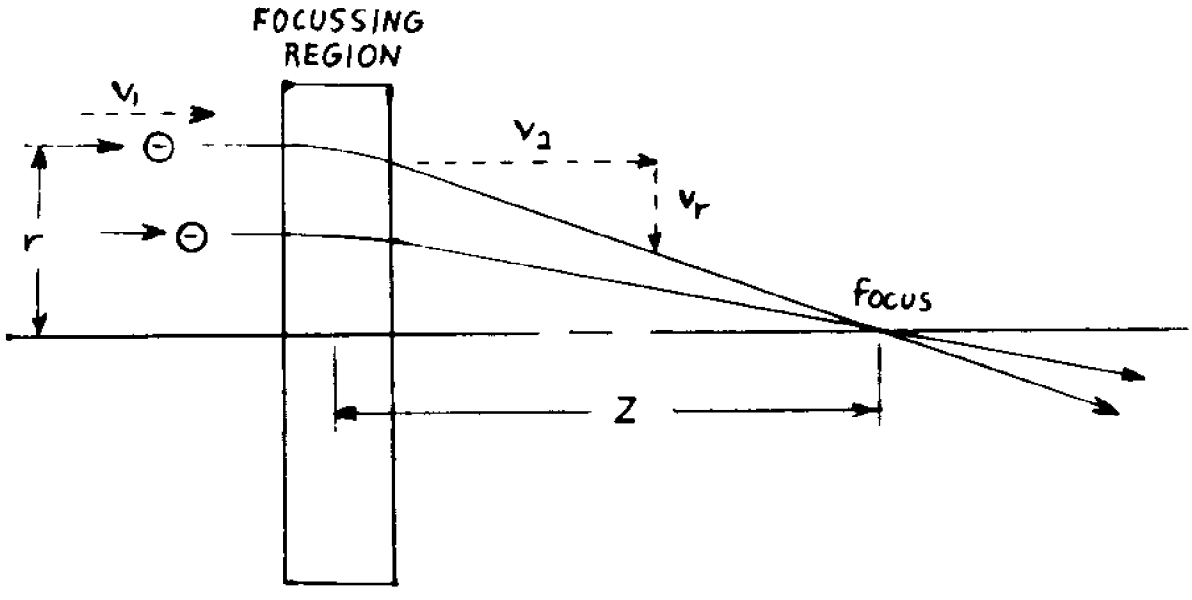

Since the electron leaves the focussing region at radius r with an axial velocity v_2 and an acquired radial velocity v_r, it follows from simple geometric considerations that:

(IV-5) $$z = r(v_2/v_r)$$

where r is the initial distance of the paraxial electron from the axis, and z is the distance of the focus point from the center of the lens.

Note that the same radial velocity is imparted if the lens if employed to accelerate an electron from potential V_1 to V_2, or to decelerate an electron from potential V_2 to V_1. As a result, the focal length of the lens depends upon whether the lens is accelerating or decelerating, and is proportional to the velocity at which the electron leaves the lens.

For a thin lens, in which the energy imparted to the electron ($V_2-V_1 = \Delta V$) is significantly less than the average kinetic energy of the electron as it passes through the lens, it is possible to show, using Eqns. (IV-4), (IV-5) and substituting for E_a ($E_a = \Delta V/d$, where d is the distance between the electrodes), that

(IV-6) $$z = 8(V/\Delta V)^2 d$$

Eq. (IV-6) underestimates the focussing power of the lens. In actual practice, with "thick" lenses, and with apertures which are not very small, the ability of the lens to focus electrons to a focal point remains unimpaired, although the focal length of the lens is considerably shorter than is anticipated on the basis of "thin lens" calculations.

Furthermore, Eq. (IV-6) illustrates several important points, which are generally true for all electron lenses. Note that the focal length

of the lens is not an absolute value, but depends upon the dimensions of the lens. Hence, the focussing properties of the lens (or a series of lenses) remains invarient with any change of scale.

In addition, Eq. (IV-6) shows that the focussing of the lens depends only upon the relative potentials applied to the electrodes. This is strictly true only when the electron beam is monoenergetic, and in actual practice, the energy spread of an electron beam (typically less than 1 eV for electrons emitted from a thermionic cathode) is usually negligible compared to the potentials applied to lens electrodes. As a result, a lens which accelerates an electron beam from 50 to 100 electron volts energy has the same focussing properties as does a lens which accelerates the beam from 500 to 1,000 eV. In other words, the focussing of a lens (or series of lenses) depends only upon the ratio of potentials applied to the electrodes.

The basic two-aperture lens previously described provides two effects which need to be considered in the design of a lens system.

(1) The electron beam is altered in kinetic energy upon passing through the lens.

(2) The electron beam undergoes a convergent focussing action. These two functions may not be varied independently, which limits the usefulness of the simple two-aperture lens. The design of an electron-optical focussing system is considerably simplified by the use of lens elements whose focussing properties and beam acceleration may be independently varied.

A three-aperture lens operated so that electrons are successively accelerated and then decelerated, leaving the focussing region at the

same potential as they entered, is characterized by no net change in beam energy within the lens. Nonetheless, in passing through the successive accelerating and decelerating electric fields, electrons experience a net radial acceleration toward the axis. This type of lens, in which an electron enters and leaves the lens with the same kinetic energy, is known as a "unipotential lens" (it is also referred to as an Einzel lens).

The focussing action of a unipotential lens is adjusted by varying the potential on the central lens electrode. Obviously, if no potential difference is applied between the central and outer electrodes ($V_1 = V_2$), then electrons are not exposed to any electric field within the lens, and the entire lens acts as a field-free region, devoid of any focussing action. As a small potential difference is applied between the central and outer electrodes, an electron will be slightly focussed toward the

FIG. (17) Cross Section of a unipotential aperture lens

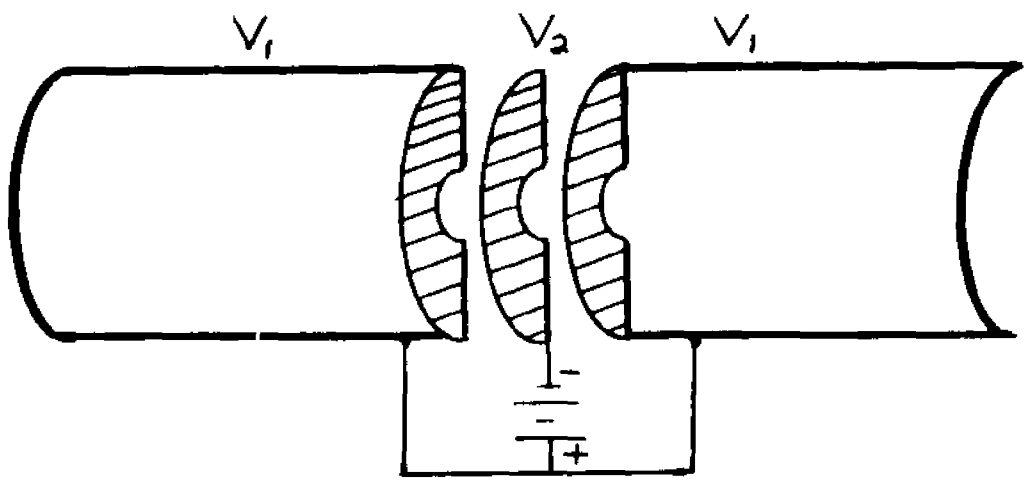

axis, and the focussing region acts as a thin lens. By increasing the potential difference, the converging action progressively increases (i.e., the focal length decreases). It is curious to note that any

potential difference, positive or negative, between the central and outer electrodes, will result in a convergent focussing of the electron beam. Usually in fact, the central electrode is operated at a lower potential than the outer electrodes so that the minimum voltage is required to achieve the desired focussing. By the use of a unipotential lens, the focussing action can be continuously varied (from non-focussing at $V_1 = V_2$ to strong focussing at either $V_1 >> V_2$, or $V_2 >> V_1$) by adjusting only the potential of the central electrode.

The origin of the focussing action of an aperture lens follows as a simple extension of the theory applied to the two aperture lens. More detailed and accurate calculations to derive the focussing properties of aperture unipotential lenses is described by Read[42].

Another useful type of lens element is a system capable of accelerating or decelerating an electron beam over a wide range of electron kinetic energies, while maintaining constant focussing characteristics. Such a lens element has been referred to as a "zoom lens", since the operation is somewhat analogous to the operation of optical zoom lenses. The analogy however is not rigorously valid, though the lack of a more suitable term compels the author to adopt this expression. An understanding of the operation of zoom lenses is not as straightforward as for unipotential lenses, although it is clear that in a three-electrode lens in which the potentials of the outer electrodes are specified, some value of the potential on the inner electrode will uniquely allow any desired focussing to be achieved. Calculations investigating the properties of zoom lenses have been undertaken as applied to 3-electrode[43] and 4-electrode[44] cylinder lenses.

Cylinder Lenses

An electron lens utilizing the electric field generated when a potential difference is applied between two adjacent cylinders on the same axis is referred to as a cylinder lens. This in fact may be viewed as a limiting case of the aperture lens depicted in fig. (14) with large aperture diameters. The electric field within the lens is essentially localized to the region near the junction of the cylinders, penetrating a distance of less than one aperture diameter into the otherwise field-free region within each cylinder.

Fig. (18) Cutaway Drawing of an accelerating Cylinder Lens

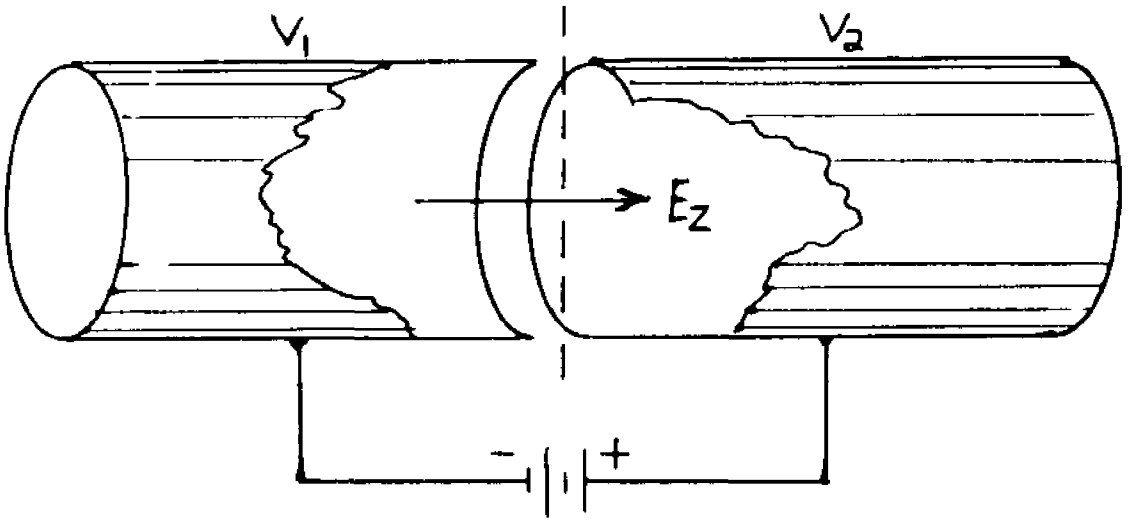

The accelerating force near the axis of a cylinder lens has been thoroughly investigated. To a good approximation, it has been determined that the electric field component parallel to the axis E_z at Z distance from the central plane of the lens (midway between the two cylinders and

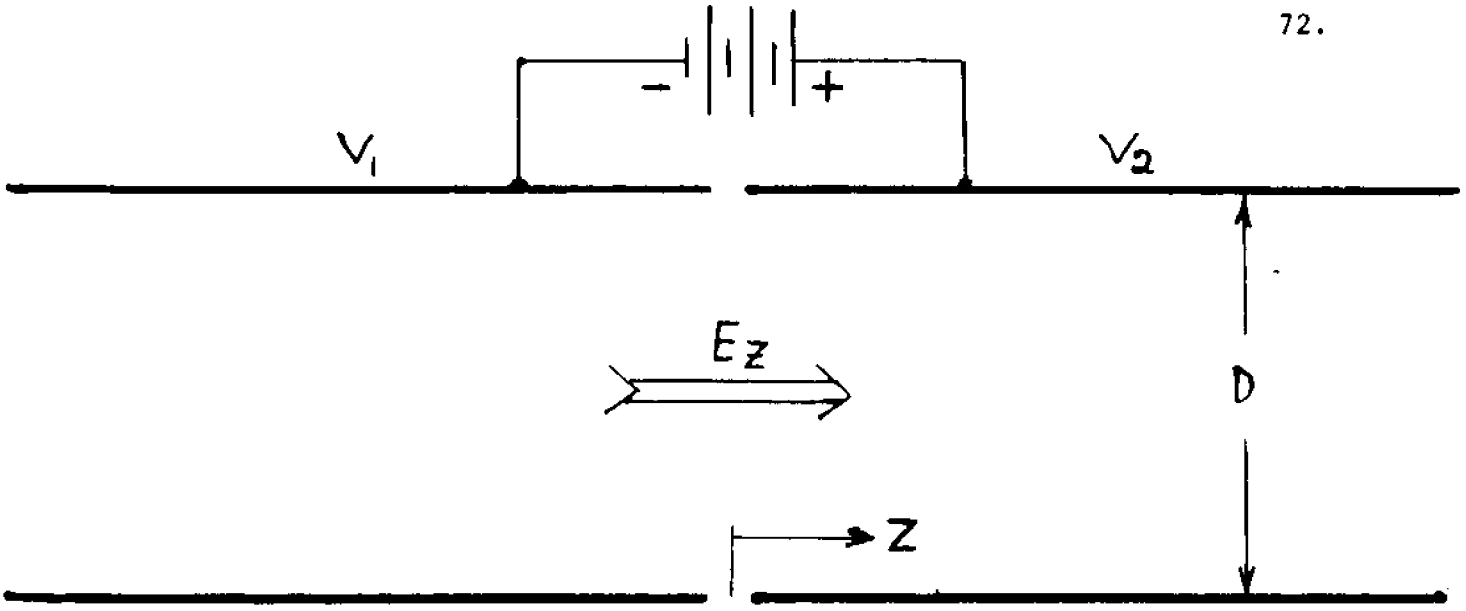

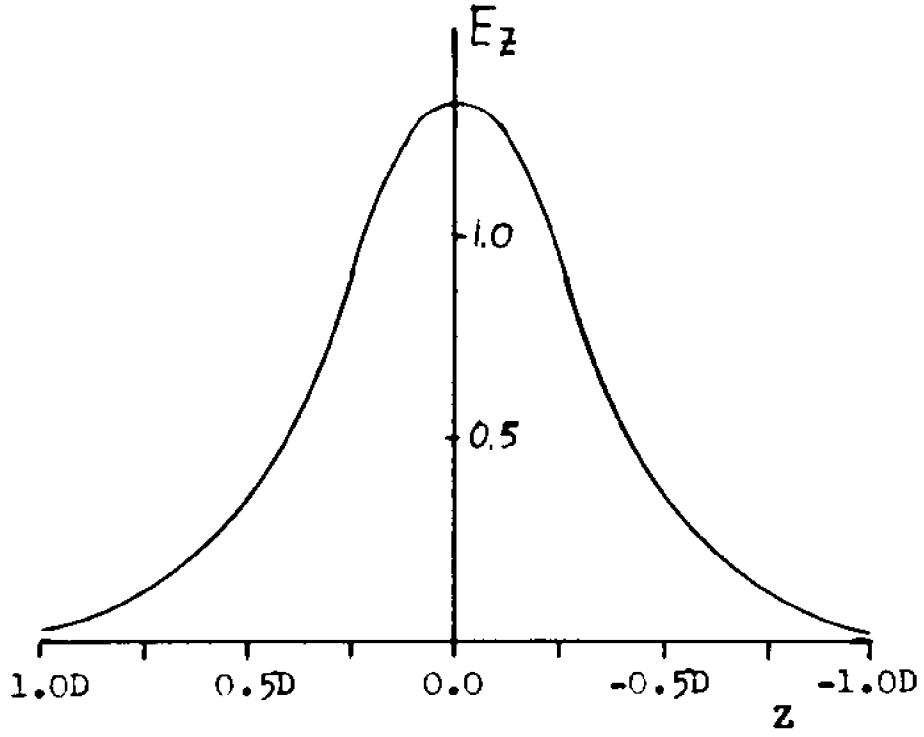

E_z is in units of $(V_2-V_1)/D$

Figure(19) The axial Electric Field E_z within a Cylinder Lens

perpendicular to the axis) is given by

$$(IV\text{-}7) \qquad E_z = (1.315)\left(\frac{V_2-V_1}{D}\right)\operatorname{sech}^2\left(\frac{2.63Z}{D}\right)$$

where D is the diameter of the lens cylinders.

Eq. (IV-7) is only valid near the axis of the lens. Electrons traveling at large radial distances from the axis, if allowed to enter the lens, are subject to a distortion referred to as spherical aberration. The use of apertures or windows are required to restrict electrons entering the lens to those within small radial distances (considerably less than the radius of the lens cylinders).

The variation of the electric field E_z from the central plane of the lens is plotted in Fig. (19). It is apparent, as would be expected, that the maximum electric field component parallel to the axis is present at the central plane of the lens. As the distance Z from the central plane is increased, the magnitude of the electric field E_z decreases, becoming insignificant at a distance of one cylinder diameter from the central plane.

We may consider the plight of a paraxial electron hurling through the field-free region of the cylindrical electrode, about to experience the accelerating and radial focussing forces within the focussing region. Once again, attention will be restricted to the concept of thin lens operation ($V_2-V_1 \ll V_1$), an oasis of mathematical simplicity. In this case, the forces experienced by the electron in its journey through the focussing region act merely as a small perturbation, only slightly affecting its trajectory within the lens.

In addition to the accelerating field E_z, an electron approaching the central plane experiences a converging radial field E_1. By using Gauss's law, the field, E_1, present at radius r at a distance Z from the central plane of the lens can be determined.

Envision a hypothetical disc-like volume element of radius r and thickness ΔZ situated concentric with the axis of the lens. Because no charge is located within the volume element (with the exception of the space charge of the electron beam), Gauss's law requires the total electric field flux diverging from the volume element to be zero. Since the axial electric field increases at points nearer to the central plane of the lens, at the inner disc surface (nearer to the central plane) the axial field is greater than at the outer surface by $(dE_z/dZ)\Delta Z$. The net field flux flowing out of the faces of the disc, $(dE_z/dZ)\Delta Z(\pi r^2)$ must be equal to the radial flux entering the periphery of the disc.

Fig. (20) A hypothetical disc-like volume element of radius r at distance Z from the central plane of the lens.

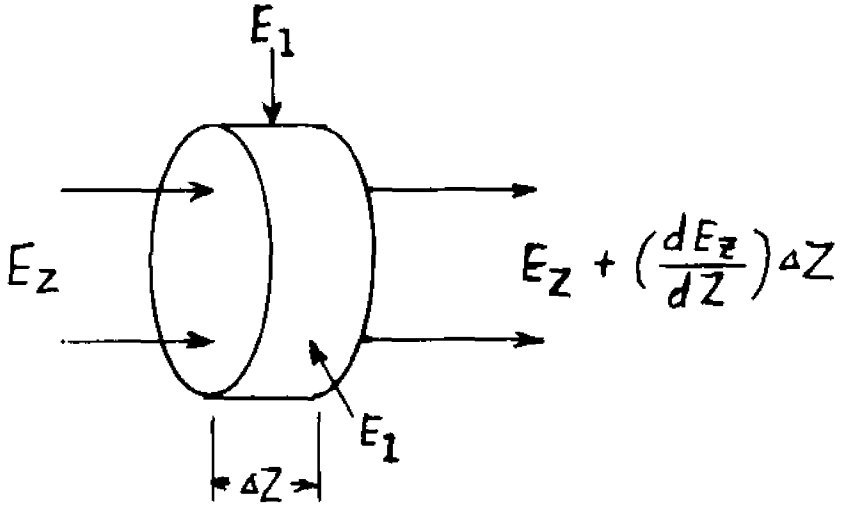

$$[dE_z/dZ)\Delta Z]\ \pi r^2 = E_1\ (2\pi r \Delta Z)$$

simplifying,

$$E_1 = \tfrac{1}{2}(dE_z/dZ)r \qquad \text{(IV-8)}$$

Upon traveling distance ΔZ, the impulse of force E_l acting on the electron for time $(\Delta Z/v_a)$ imparts a radial velocity Δv_r toward the axis.

$$E_l(\Delta Z/v_a) = m_e \Delta v_r$$

$$\Delta v_r = E_l \Delta Z/m_e v_a \qquad \text{(IV-9)}$$

The total radial velocity imparted to the electron in transversing the focussing region of the lens may be determined by integrating the radial velocities acquired in each distance element ΔZ within the focussing region. It is curious to note however, that while the radial force is converging as the electron approaches the central lens plane, it is diverging on the other side of the plane. Furthermore, the symmetry of the lens requires that the radial electric fields E_l on opposite sides of the central plane (at the same radius and same distance Z) are exactly equal in magnitude and opposite in direction. Initially, it might appear that the conv erging effect of one half of the focussing region is exactly compensated by the diverging action on the other side of the central lens plane. This is not the case however, and the net effect of the cylinder lens is converging due to two factors:

(1) Within the initial coverging region of the lens, the electron is traveling with a smaller axial velocity than it will have after being accelerated to the diverging portion of the focussing region. Hence, the converging force acts on the electron for a longer period of time, and imparts a higher radial velocity.

(2) The initial converging field accelerates the electron inward to a smaller radius, so that upon entering the diverging region, the outward radial field will be decreased.

Cylinder lenses which are decelerating can also be shown by similar reasoning to have a net converging effect. Regardless of the direction with which a paraxial electron enters the lens, the same inward velocity is imparted within the focussing region. Furthermore, because the radial velocity imparted to electrons is proportional to their radius, all paraxial electrons leave the focussing region converging toward a focal point.

Bear in mind that an analysis involving paraxial electrons is merely a convenient concept. Electrons moving exactly parallel connotes an infinitesimal angular divergence of the beam, and hence, a beam of either infinite brightness or zero intensity. The ability of an electron lens to focus electrons to a point, or to an undistorted image, depends upon the angular range accepted into the lens (just as the sharpness of focussing and depth of field of a camera lens are enhanced by the use of a narrow aperture to restrict the angular range of light accepted into the lens from each point in a light source). For while a lens system allows desired focussing properties to be attained, the operating characteristics must be within the bounds of optical laws.

V. PHOTOIONIZATION AND THERMIONIC ELECTRON SOURCES

Much of the field of electron spectroscopy is based upon the generation of electrons resulting from the photoelectric effect. Photoionization can occur whenever molecules are irradiated with ultraviolet or X-Ray radiation of sufficiently high energy to eject electrons from the molecular orbitals of the molecule. The difference between the energy of the incident photon (E=hv) and the ionization potential of the molecular orbital from which an electron is ejected appears as kinetic energy of the resulting electron. A measurement of the kinetic energies of photoelectrons emitted from a chemical sample allows information about the orbital energies and bonding of the molecule to be directly obtained. This instrumental technique, known as photoelectron spectroscopy, utilizes a high energy monochromatic radiation source to irradiate a sample, and a system to energy analyze the resulting photoelectrons.

Since its inception less than twenty years ago, photoelectron spectroscopy has evolved along two diverging paths. While the two forms of instruments which have emerged, Vacuum ultraviolet (VUV) and X-Ray photoelectron spectrometers, are nearly identical in operation, the information provided about the chemical sample under study is entirely different. For while orbitals of low ionization potential are intimitely involved with the bonding of the molecule, inner shell orbitals of high ionization potential are essentially localized near atomic nucleii and affected only by the immediate atomic environment.

VUV photoelectron spectroscopy uses vacuum ultraviolet radiation of relatively low energy to investigate molecular orbitals of low ionization

potential. The gas discharge radiation sources (the 21.21 eV resonance emission from helium is used predominently) are almost invariably windowless, requiring differential pumping in order to minimize the gas load effusing into the main vacuum chamber. As a consequence, little emphasis is placed upon the attainment of very high vacuum, since a vacuum much better than 10^{-5} torr is neither required, nor readily attainable.

An examination of the VUV photoelectron spectrum of a chemical compound provides the energy states of delocalized molecular orbitals of low ionization potential. The VUV photoelectron spectra of some simple molecules have been compiled and analyzed by Turner et al[13]. Subsequent to the publication of this classic reference, the VUV photoelectron spectra of many more molecules have been obtained and published in various journals.

X-Ray photoelectron spectroscopy (also referred to as ESCA) employs high energy (generally x-ray resonance source with photon energies of about 1,000 eV are employed) capable of ejecting electrons from orbitals of high ionization potential. Such inner shell electrons retain the characteristics of atomic orbitals, whose energies are only affected to a minor degree by the molecular environment of the atom. As a result, x-ray photoelectron spectra are predominantly determined by the types of atoms present in the sample, with subtle "chemical shifts" belieing the chemical environment of each atom within the molecule. The sample generally consists of a solid, from which only electrons near the surface (less than about 50A deep) can escape. As a result, ultrahigh vacuum conditions (about 10^{-8} torr) are often required in order to avoid contamination of the surface. Much of the development of the technique and literature published[45] is directly attributed to K. Siegbahn and coworkers.

A secondary process associated with photoionization of inner shell electrons, upon which another from of electron spectroscopy has been based, is the Auger effect. Once a molecule has undergone photoionization of an inner electron, the remaining ion is left in a highly excited state. In order to relax to the ground state of the ion, two processes compete for the dissipation of the excess energy. The first process, which predominates for heavy nucleii of atomic number greater than 12, is x-ray fluorescence. For light nucleii of atomic number less than 12, the primary process for the release of excitation energy is the ejection of another electron, resulting in a doubly ionized ion. The energies of such Auger electrons depend primarily upon the element involved, with a subtle dependence upon the molecule environment of the atom. Auger spectrometers may rely upon x-ray irradiation of the sample to form the highly excited ions, or upon the excitation by electron impact. A complete chart of Auger electron energies for various elements is available from Physical Electrons Inc., a manufacturer of electron impact Auger spectrometers.

Fig. (21) The Process of Auger Electron Ejection

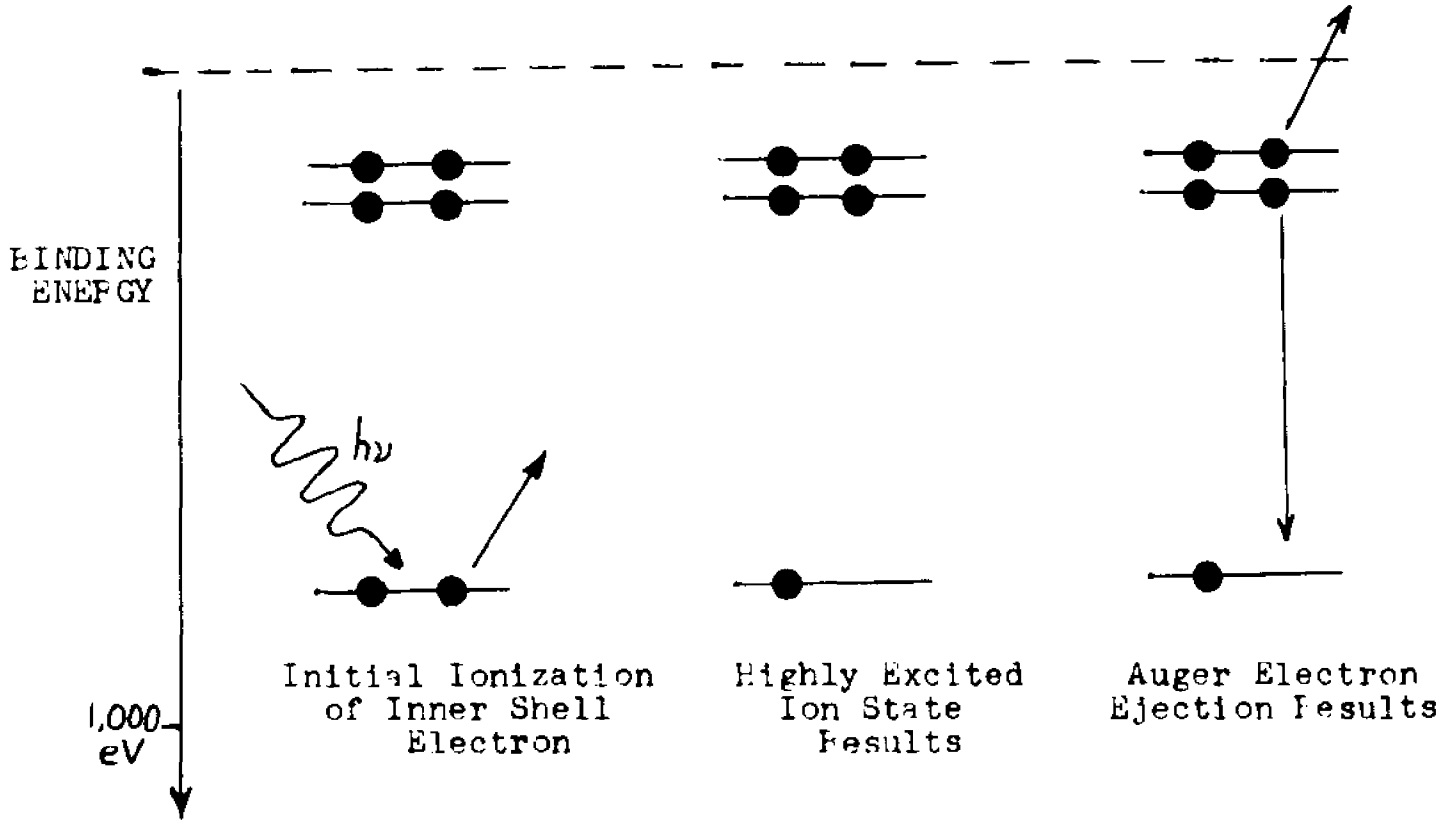

Subtle structure in Auger spectra due to the involvement of outer shell electrons has also been investigated for simple gaseous molecules[46].

VUV Radiation Sources

Common VUV radiation sources utilize an electrical discharge within a low pressure inert gas. Among the many processes occurring within the discharge is excitation, resulting in the emission of VUV radiation upon relaxation to the ground state. Due to the long lifetime of the excited state, resonance radiation from discharge lamps is generally highly monochromatic. This is a most useful feature of the radiation, since, by choosing the proper gas, monochromatic VUV radiation of a desired photon energy generally can be obtained. Table (I) lists the major resonance emissions of the inert gases. For radiation of photon energy below 11.9

eV, it is possible to use a window of LiF, or several other possible window materials so that the lamp may be sealed, and thus eliminating all difficulties associated with differential pumping.

Lithium fluoride is a rather remarkable and unique material. It is transparent to radiation of all energies, from the far infrared region through the visible and ultraviolet range, up to the cutoff energy of 11.9 eV in the vacuum ultraviolet region. The material is limited however in that its transmission in the VUV is adversely affected by humidity, and gradually diminishes upon exposure to VUV radiation (after a rapid initial dropoff in transmission). Although windows of thin layers (1500A thick) of aluminum have been proposed for HeI radiation (21.21 eV photon energy), considerably above the cutoff of LiF, these windows are subject to extreme mechanical fragility and highly susceptible to corrosion by moisture or chemical vapors. Therefore, it appears that as of this writing, LiF has the highest energy cutoff of any viable, commercially-available material.

Another useful and commercially available window material is MgF_2, with a slightly lower photon energy cutoff of 11.2 eV. Besides the lower energy cutoff, MgF_2 offers superior properties as a window material. It is virtually invulnerable to exposure to moisture (transmission remained nearly unaffected after soaking in water for 24 hours), and does not undergo the gradual deterioration of transmission upon exposure to VUV radiation that characterizes LiF. The material is reasonably mechanically robust, may be heated to 500°C without damage (although all window materials of LiF, MgF_2 and CaF_2 are subject to cracking if heated or cooled rapidly), and is reasonable in price ($25 for a half inch diameter window, as of Dec. 1975 from Harshaw Chemical Co., Crystal & Electronic Prod. Dept.,

TABLE I RESONANCE VUV DISCHARGE SOURCES

Gas	Main Resonance Emission, eV	Possible windows*
He	21.21	None
Ne	16.85 16.67	None
Ar	11.83 11.62	LiF
Kr	10.64 10.03	LiF, MgF_2
Xe	9.57 8.44	LiF, MgF_2, CaF_2

Window Cutoff Energies

LiF	11.9 eV
MgF_2	11.2 eV
CaF_2	9.9 eV

*Excluding thin films. See text.

Solon, Ohio 44139). In view of these properties, it appears remarkable to the author that windowed VUV lamps have not completely displaced differentially pumped discharge lamps where photon energies below 11.9 eV are adequate.

All VUV sources are highly inefficient compared to conventional visible and ultraviolet sources. In part, this is due to the requirement of photoelectron experiments that the lamp form a narrow, well collimated beam. However, even despite the loss of VUV flux resulting from collimation of the beam, the process of generating VUV photons itself appears to be quite inefficient. Most likely the long lifetime of the excited state, which is responsible for the narrow bandwith of the emitted radiation, results in the inability to compete successfully with the emission of infrared, visible and UV radiation, where excited state lifetimes are much shorter. A typical output of a VUV discharge source is about $5X10^{10}$ photons/second, or a radiation energy of the order of 10^{-7} watts. For a discharge lamp whose energy input is in the range of 10 watts, the overall efficiency for the production of VUV radiation is a rather unimpressive 10^{-6}%. This output is often quite adequate for most experiments, although an attempt to study photochemical reactions induced by VUV radiation would be restricted to photochemical chain reactions of very high quantum efficiency, or to experimenters with an inordinate degree of patience.

In addition to the field of electron spectroscopy, compact VUV sources have potential for application in other areas. Since only certain molecules have a sufficiently low ionization potential to be ionized by by resonance radiation transmitted through a window, only certain molecules

will be subject to photoionization. Other molecules of high ionization potential, such as Helium, nitrogen, and all natural components of air will not be ionized to any degree. Those compounds which are ionizable with a given resonance radiation form a distinct group, and photoionization may be used as a sensitive means of detection of these compounds, with no response at all to compounds of high ionization potential. Consequently, photoionization has been proposed for use as a detector in gas chromatography[47] (many organic compounds, particularly aromatics, have low ionization potentials and are ionized by Kr radiation). Other work[48] with which the author is personally acquainted clearly indicates that a photoionization detector for liquid chromatography offers wide applicability and superior sensitivity, since most solvents used as a mobile phase in liquid chromatography have high ionization potentials and do not interfere in the detection of eluents.

Another possible application of a compact VUV source would be for photoionization mass spectroscopy. Since electron impact mass spectrometers are generally characterized by extensive fragmentation of the sample molecules due to the high energy of the ionizing source, as well as pyrolysis of the sample on the hot thermionic cathode, electron impact mass spectra are often quite complex and difficult for the average chemist to interpret. Photoionization with low energy radiation, on the other hand, results in much less fragmentation so that simpler spectra are obtained with enhancement of the parent peak[49] (for a review of photoionization mass spectrometry, see ref. 50). Such a mass spectrometer would probably be simpler to construct, since the ionization source would be entirely external to the ionization region, isolated by the window.

One final application, with which the author has been concerned, is a vacuum leak detector. Since all components of air undergo no ionization upon irradiation with a windowed VUV source (the ionization potentials of N_2, O_2, CO_2 and H_2O are respectively 15.5, 12.0, 13.7 and 12.6 eV), while organic compounds may be detected with high sensitivity by photoionization, an ideal means of locating leaks in a vacuum system is potentially present. Upon application of a material of low ionization potential (benzene was used in initial experiments) to a joint or area suspected of leaking, an indication of photoionization of the vapors inside the vacuum chamber unambiguously confirms that a leak is present at the point of application. Experiments performed so far indicate that such a system could be made quite compact to be permenantly mounted inside a vacuum system (in the backing line of a diffusion pump) and could probably be manufactured at a significantly lower cost than mass spectrometer leak detectors currently in use. This method of leak detection however currently offers considerably lower sensitivity than mass spectrometer leak detectors, and a material with a lower toxicity than benzene (or other similar organics) would definitely be desirable. Utilizing a sealed, radiofrequency discharge source (described later in this chapter), the photoionization current detected per unit gas leakage was about $5X10^{-8}$ amperes/(atm-cm^3/sec). Thus far, the smallest leak which could reliably be detected was an air leak resulting in a pressure of $2X10^{-6}$ torr. At this point, there seems little doubt that the attainable sensitivity of the technique could be substantially increased, and the major impendiment to the adoption of a photoionization leak detector for general use may possibly be the lack of a suitable non-toxic gas or liquid of low ionization potential.

A VUV source may use either a direct current glow discharge, a radio-frequency dischange, or microwave excitation[51] of the gas. Extensive work has been done early in this century examining the characteristics of direct current discharges, and probably because they have been so extensively studied and comprehensive literature is available[52-55], direct current discharges continue to be developed[56,57] and used to generate VUV radiation. Although such discharges are suitable for windowless, differentially pumped discharge sources, in which gas is continuously bled into the lamp, direct current discharges appear to be inadequate for sealed, windowed lamps due to gradual contamination of the gas. Since VUV lamps are generally operated at low pressure (about 1 Torr) to minimize self absorption of radiation by the gas, a small amount of contaminant gas will supress the emission of the desired VUV radiation.

During the operation of a direct current discharge, impact of positive ions on the cathode will result in the ejection of metal atoms from the surface of the electrode, referred to as sputtering. As the discharge is operated, material is continuously sputtered, depositing a metallic film of electrode material on any nearby surface. Sputtering may be visibly observed after an hour of operation on the inside walls of a hlass discharge tube operated at low pressure. Not only does the sputtering process release gases which have been dissolved in the metal during its manufacture, but more important, results in the removal of gas from the discharge tube. Positive ions formed from the gas in the discharge are accelerated toward the cathode and upon impact are injected into the electrode surface. Ions injected into the cathode will ultimately be released as the cathode surface continues to sputter, however, ions

injected into the sputtered surface will be buried underneath new deposits of sputtered material, and permanently removed from the discharge. The net effect of sputtering is to gradually remove gas from the discharge tube. This effect in a direct current discharge, known as gas cleanup, has been investigated by Bartholomew et al[58,59].

The rate of sputtering, and hence the rate of gas cleanup, depends primarily upon the pressure of the gas, the atomic weight of the gas (sputtering is lowest for heaviest ions) and the metal present in the electrode. Sputtering yields for most metals have been obtained for impact by He^{+60}, Ne^{+61}, Ar^{+61}, Kr^{+60}, Xe^{+60} and Hg^{+62} ions. These yields should be interpreted with some caution, since it is shown that the sputtering yield depends very strongly upon the kinetic energy of the impacting ion, and that in turn is determined by the electric field near the cathode under actual discharge conditions, which varies considerably with the choice of electrode. Nonetheless, this work clearly indicates that the electrode materials with the lowest sputtering yield are carbon, silicon, titanium, beryllium, niobium and vanadium (with sputtering yields of less than 0.25 atoms ejected/ion impacted for impact by 200eV Kr^{+} ions), and the worst sputterers are copper, palladium, gold and silver (with sputtering yields of more than 0.75 atoms ejected/ion under the same conditions). However, even with electrodes of low sputtering yields and free of dissolved gases, it appears that any sealed low pressure direct current discharge is subject to a very limited useful lifetime before pressure instabilities or gas cleanup make it unuseable. Difficulties associated with sputtering and gas cleanup however are eliminated in radiofrequency and microwave discharges, which have no electrodes in contact with the gas.

Due to the availability of microwave generators, microwave generators, microwave discharge VUV sources have become increasingly popular. Several papers have been published detailing the procedures for preparing lamps[63], and the use of waveguides and cavities[64] to excite the discharge. However, the inherent danger of working with microwave sources, as well as their substantial cost and size have undoubtedly discouraged some workers in the field (the author for example).

By comparison with direct current and microwave VUV sources, radio-frequency sources appear to be far more suitable in that they pose no radiation hazard, and considerable freedom exists in choosing the power capability of the generator. Surprisingly though, a search through the chemical literature revealed an incredible dearth of information on the use of radiofrequency discharges to generate VUV radiation. Most of the few available references[65-67] were concerned with the use of RF discharges to generate visible or infrared radiation.

Probably the simplest and best method of coupling radiofrequency power into a discharge is to construct a RF generator with an accessible oscillator coil, so that the discharge tube could be directly subject to the radiofrequency field within the coil. In order to do this, the circuit of a radiofrequency generator used for exciting visible emission from alkali metal vapors[66] was modified. The circuit, a high frequency astable multivibrator, is remarkably simple, inexpensive to build, and yet found to be highly effective for the generation of VUV radiation in a low pressure kryption or Argon discharge.

The circuit (shown in Fig. (22) was constructed inside a 6"X3"X2"

aluminum minibox with the coils mounted so that the discharge tube could be slid into the box through the coils. Each coil was made from 4½ turns of #18 copper wire wound on an aluminum rod slightly less than ½" diameter. Both coils were would in the same direction and mounted on opposite sides of a phenolic panel, spaced about 3/16" apart. Because of the very high frequency at which the circuit oscillates, all wiring leads were kept as short as possible.

Fig. (22) Circuit of RF generator for VUV Discharge

*The circuit may also be wired using a 6J6 dual triode, with a +250 volt plate supply.

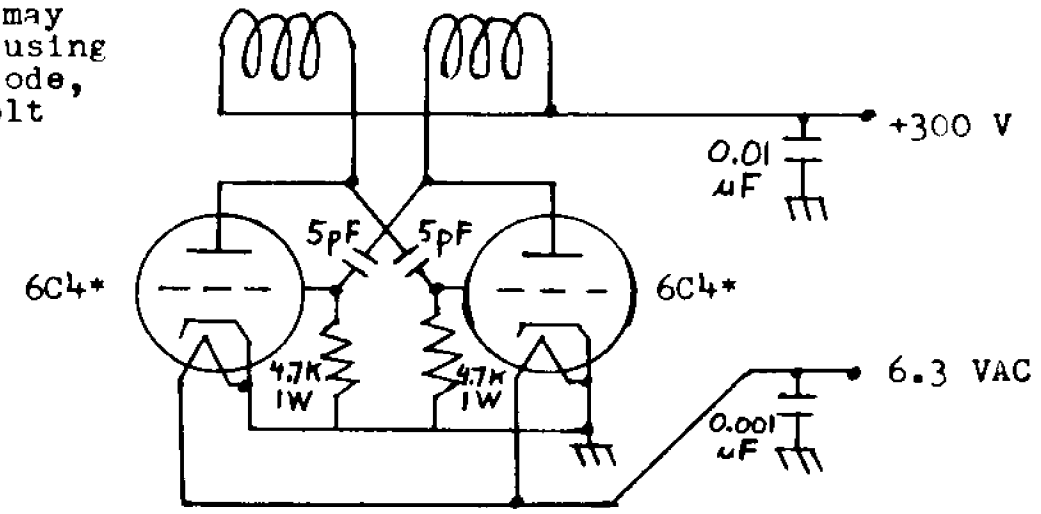

Of the 10 watt power input to the oscillator, it is crudely estimated that the power dissipated in the discharge is about 2 watts. As a VUV source, the discharge was capable of inducing a photoionization current of about $4X10^{-9}$ ampere, so that a photon output of $5X10^{10}$ photons/second is estimated.

The VUV output of the lamp increases with krypton pressure until a broad plateau is reached, at which the output remains independent of pressure. However, at higher pressures, more stringent conditions are required to initiate the discharge. It becomes necessary to increase the voltage on the oscillator, or to use a tesla coil in order for breakdown of the gas to

begin. The region occupied by the discharge varies with the krypton pressure, being diffuse at low pressures and withdrawing at higher pressures into the area directly within the oscillator coil.

The discharge tube itself is basically a 10 mm O.D. pyrex tube terminating in a pyrex flange. Using carborundum powder (120 grits), the flange is ground flat, or ground to contain a seat for the window. Epoxy resin may be used to seal the window to the flange, although sealing with AgCl as provided by a relatively simple procedure[68] would allow operation at high temperatures (in excess of 300°C.) and probably provide a more reliable seal. An aluminum backup flange presses the glass flange against a mating flange with an O'ring, sealing the lamp to the desired ionization region.

Thermionic Emission

Electron emission from the surface of a metal at room temperature is normally precluded by the existence of a potential energy barrier within several atomic diameters of the surface. Upon heating the metal, the kinetic energy of the electrons will increase so that a small fraction impinges upon the surface energy barrier with sufficient energy to escape from the metal surface. Such a process of thermionic emission allows some pure metals and specially prepared composite surfaces to be used as electron sources. In order for thermionic emission to occur to a significant degree, the metal surface must be characterized by a relatively low energy barrier for escape, referred to as the work function, and by a high melting point so as to allow the metal to be heated to very high temperature without melting or undergoing gradual vaporization. These requirements limit the use of pure metal thermionic emitters to several elements, most

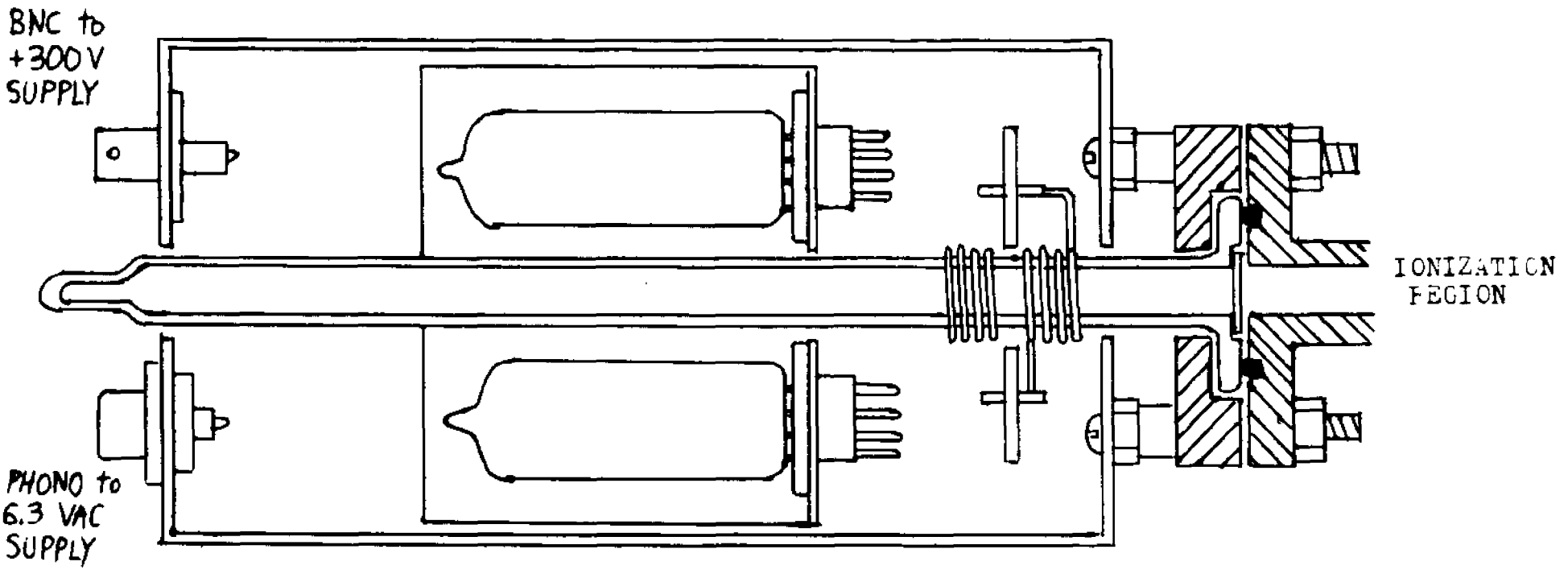

Figure(23) RF Discharge VUV Source, showing major components
(appr. actual size)

notably tungsten (work function of 4.5 eV, melting point 3,410°C.).

The surface of a thermionic cathode need not be composed of pure metal, and extensive work has led to the development of various surfaces impregnated with metals or metal oxides of low work function. These composite cathodes are often indirectly heated by a separate tungsten heater, electrically insulated from the cathode.

Generally, as the operating temperature of the thermionic cathode is increased, the emission substantially increases (typically doubling for a 50°C. increase in temperature), although the useful lifetime of the cathode decreases. Consequently. some compromise must be chosen for the optimal temperature at which the cathode is operated. In considering the suitability of different types of thermionic cathodes, it is necessary to compare the operating lifetime at which a specified emission is obtained, as well as other important characteristics.

For cathodes used in electron spectrometers, susceptibility to poisoning is a particularly relevant consideration. Various types of cathodes differ over an extreme range in the ability to resist poisoning of the surface. Oxide coated cathodes (commonly used in electronic vacuum tubes), once chemically activated by initial heating to above operating temperature, are highly vulnerable to poisoning by exposure to gas. Even momentary exposure of an activated oxide cathode to air irreversibly alters the nature of the cathode surface, decreasing the emission to the extent that it becomes useless as a thermionic emitter.

Barium impregnated tungsten cathodes, on the other hand, are relatively insensitive to poisoning. Such cathodes may be exposed to the atmosphere

when cool (although extensive contact with humid air should be avoided) and do not require a complicated activation procedure. Technical information on barium impregnated cathodes is available from the manufacturer, the Philip Elmet Corp., 1560 Lisbon Road, Lewiston, Maine 04240. Type BP-1A cathodes are the least vulnerable to poisoning and have been used successfully in electron impact-energy loss experiments[69], and experience by the author has confirmed that such cathodes do provide high emission, low sensitivity to poisoning, and are simple to activate and use. The cathodes may be ordered with a tantalum wire spot welded to the cathode case as a means of mechanically supporting the hot (1150^{o}C.) cathode.

Directly heated wires of tungsten or thoriated tungsten are probably the least sensitive to poisoning. Such bonded thoria filaments are commonly employed in Bayard-Alpert pressure gauges, and are available as standard filaments for these gauges (from Electron Technology Inc., 636 Schuyler Ave., Kearney, N. J. 07032).[70]

Considerable higher emission than is available from conventional cathodes, at the same operating lifetime, has recently become commercially available (at higher initial cost) with LaB_6 cathodes (from Kimball Physics Inc., Wilton, N. H. 03086).

The maximum current density which may be emitted by a thermionic cathode, known as the saturation current, is given by the well known equation

$$J_c = AT^2 e^{-\phi/kT} \qquad (V\text{-}1)$$

where J_c is the saturation current per unit area at the cathode surface,

$A = 4\pi m_e k^2 e/h^3 = 13$ amperes/cm^2, ^{o}K^2

T is the absolute Kelvin temperature of the cathode and ϕ is the

cathode work function.

The saturation current is only drawn from the cathode when a large electric field is applied at the cathode surface to rapidly accelerate the slow emitted electrons away from the cathode. In the absence of a large electric field, repulsion between the emitted electrons creates a space charge immediately in front of the cathode, increasing the electrical potential of that region above the potential of the cathode. Effectively, the space charge created by the emitted electrons increases the work function associated with the surface, as the escaping electrons must now have enough energy to overcome the intrinsic barrier at the cathode surface, as well as the barrier due to repulsion by other electrons near the cathode surface. The emission current from the cathode consequently is highly dependent upon the electric field applied at the cathode surface (unless the electric field is so large as to draw the saturation current from the cathode), a characteristic which has allowed thermionic electron tubes to have been widely employed as electronic amplifiers.

Electron Guns

An electron gun is a device for accelerating the low energy electrons from a cathode and focussing them into a well defined beam. An understanding of the operation of electron guns is based upon the electron optical laws outlined earlier, as well as a consideration of space charge, which often is the dominating factor in the operation and limitations of electron guns.

A thorough discussion of the design of electron guns would be quite complicated and inappropriate at this point. Several excellent references

on this topic are available[71-75]. Furthermore, rather than attempt to build an electron gun, an experimenter would be well advised to use commercially available electron guns (for use in cathode ray tubes) if at all possible. Such guns, although designed to be used at energies of 20,000 electron volts, can function at a much lower energy of about 100 volts, as experiments by the author have clearly shown. Dur to their mass production, electron guns for cathode ray tubes are available at a price which is virtually negligible (about $2 each, as of November 1973, from Apex Electronics, 100 Eighth Street, Passaic, N. J. 07055, or Arvin Automation, 1384 Pompton Avenue, Cedar Grove, N. J. 07009).

Experiments by the author with a commercially available electron gun (model 2233A, Apex Electronics) have shown that this gun may not only be operated at relatively high pressure (10^{-2} torr) without poisoning of the cathode, but that the beam current actually increases substantially at higher pressures (probably due to neutralization of space charge by positive ions). Furthermore, with the gun operating at pressures of 10^{-3} to 10^{-2} torr, the electron beam could clearly be seen in a dark room as a bluish glow, and the effect on the focussing properties brought about by changing the voltages on the electrodes clearly discerned. Although it is questionable how closely operation of the gun at these pressures simulates performance in a high vacuum (less than 10^{-6} torr), the visible observation of the electron beam allows at least semiquantitative observation to be made, and constitutes a facinating experiment.

The basic criteria of electron gun operation is the ability to form a beam of high current density in a field-free region. Two limitations are present, either or both of which ultimately determine the current

density which may be achieved.

One factor is the repulsion of electrons from the space charge created by the high density beam. While the effect of space charge often may be neglected in the consideration of energy analyzers or electron optics designed to handle low currents, the very high electron beam densities (typically 10^{-3} amperes/cm^2) characterizing the operation of electron guns results in space charge effects becoming a dominant factor.

In the formation of low energy electron beams, space charge effects near the cathode may be overcome by multistaging the gun[75], that is, extracting the electrons from the cathode with a high accelerating voltage, and then decelerating the beam to the final energy. The design of the electron gun may then be divided into two distinct parts: design of an extraction stage to draw electrons from the cathode with a high electric field, and a decelerating stage utilizing standard electron optical lenses to focus the beam to the desired energy.

The ultimate limitation of space charge is not inherent in the design of the electron gun, but rather in the characteristics of the final beam. Consider the beam to have a radius r_o within the last focussing stage, and an attempt to be made to focus the beam to a point at distance L from the last gun element. The beam will consequently be projected upon the focus point at a convergence angle ϕ. It is well known[72] that the space charge repulsion of the electron beam will spread the beam at the focus point to a radius of 0.425 r_o, and furthermore, that the current that may be projected at this convergence angle is

$$I_{max} = (38.5)\, E^{3/2} \tan^2 \phi \qquad \text{(V-2)}$$

Fig. (24)

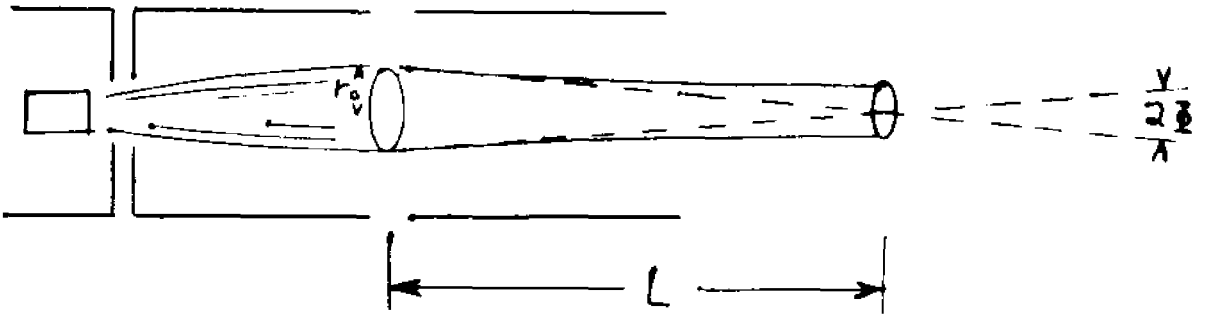

where I_{max} is the maximum current in μA

E is the beam energy in electron volts, and

Φ is the convergence angle in radians

It is interesting to note that the maximum beam density (current/unit area) allowed by space charge considerations is determined only by the final energy of the beam and the distance of the focus from the last stage of the gun.

$$(V\text{-}3) \qquad J_{max} = \frac{I_{max}}{(0.425r_o)^2} = \frac{(67.7)E^{3/2}}{L^2}$$

The space charge limit however should not be construed as an absolute limitation, nor as the factor which will necessarily determine the maximum beam density. A strong magnetic field along the axis of the beam will confine the electrons within a small radius for large distances from the gun, and Equations (V-2) and (V-3) are no longer applicable in this situation. Furthermore, in actual performance, electron guns often exceed the space charge limitation of Eq. (V-3) due to neutralization of inter-electron repulsion by the formation of positive ions within the beam resulting from ionization of residual gas. Even at pressures as low as 10^{-6} torr, the effect of positive ions may become significant. Operation

of the gun at higher gas pressures may even further reduce or eliminate the space charge restriction.

In these cases, the brightness of the cathode becomes the predominant consideration in limiting the maximum attainable beam density. Unlike space charge effects, the brightness limitation places an absolute restriction on the attainable current density in the final beam, which may not be circumvented by any instrumental design.

Electrons are emitted at a cathode surface over a hemispherical angular range, with a characteristic current density J_c determined by the composition and temperature of the cathode (as stated by Eq. (V-1)). Thermionic electrons furthermore are emitted at kinetic energies averaging approximately kT (where T is the temperature of the cathode, and k is the Boltzman constant, $8.6X10^{-5}$ eV/^{o}K), and the brightness of the beam (current/area, solid angle) may only be increased by acceleration to higher beam energy. It therefore follows that if the beam is to be focussed to a convergence angle Φ at energy E, the brightness of the cathode limits the final beam density to a value

$$J_{max} = J_c(E/kT)\sin^2\Phi \qquad (V-4)$$

Clearly, the attainment of high current densities is inherently more difficult at low beam energies, regardless of whether the gun is brightness or space charge limited. Which limitation will prevail is determined by the operation of the gun: the temperature of the cathode, and the characteristics of the final beam. Generally, it is to be expected that at low cathode temperature, the electron beam density is limited by the brightness of the cathode. As the cathode temperature is increased, the attainable current density will increase, until the gun

becomes space charge limited. The operating temperature of the cathode should then be chosen so as to provide a compromise between lifetime and current density at a temperature below the onset of space charge limited operation.

VI. ELECTRON SPECTROSCOPY COINCIDENCE EXPERIMENTS

Electron spectroscopy essentially involves the measurement of electron kinetic energy spectra resulting from particular processes of photoionization, inelastic scattering or excitation. Considerable information about the energy levels of molecules and ions has thus been derived from photoelectron, electron impact and Auger spectra.

Scanning an electron kinetic energy spectrum may thus be referred to as a one parameter experiment since only the electron kinetic energy is measured. This type of experiment is generally characterized by moderately high data collection rates at high resolution, although the extent of the information which may be obtained is limited. For while the detection of an electron of known energy reveals the state of the ion or molecule from which it was dispatched, it can yield little information about the fate of the resulting excited species. It is only after the initial process of ionization or excitation that the resulting species will embark on a chemical adventure of unimolecular fragmentation into ions, reaction with other molecules, or the emission of radiation.

A basic one parameter electron spectrometer is depicted in Fig. (25). Electrons photoejected or scattered from a sample molecule enter an energy analyzer, whose function is to transmit electrons within a kinetic energy range ΔE, while discriminating against all electrons of other energies. Of the total number of electrons produced per second, N, only a small fraction have the proper energy, and enter the analyzer with the proper orientation, to be transmitted by the analyzer and detected. The resulting signal due to electrons within energy range ΔE is:

$$S = N g f_e \Delta E \quad \text{electrons/second} \tag{VI-1}$$

Figure(25) Schematic Diagram of a One Parameter Experiment

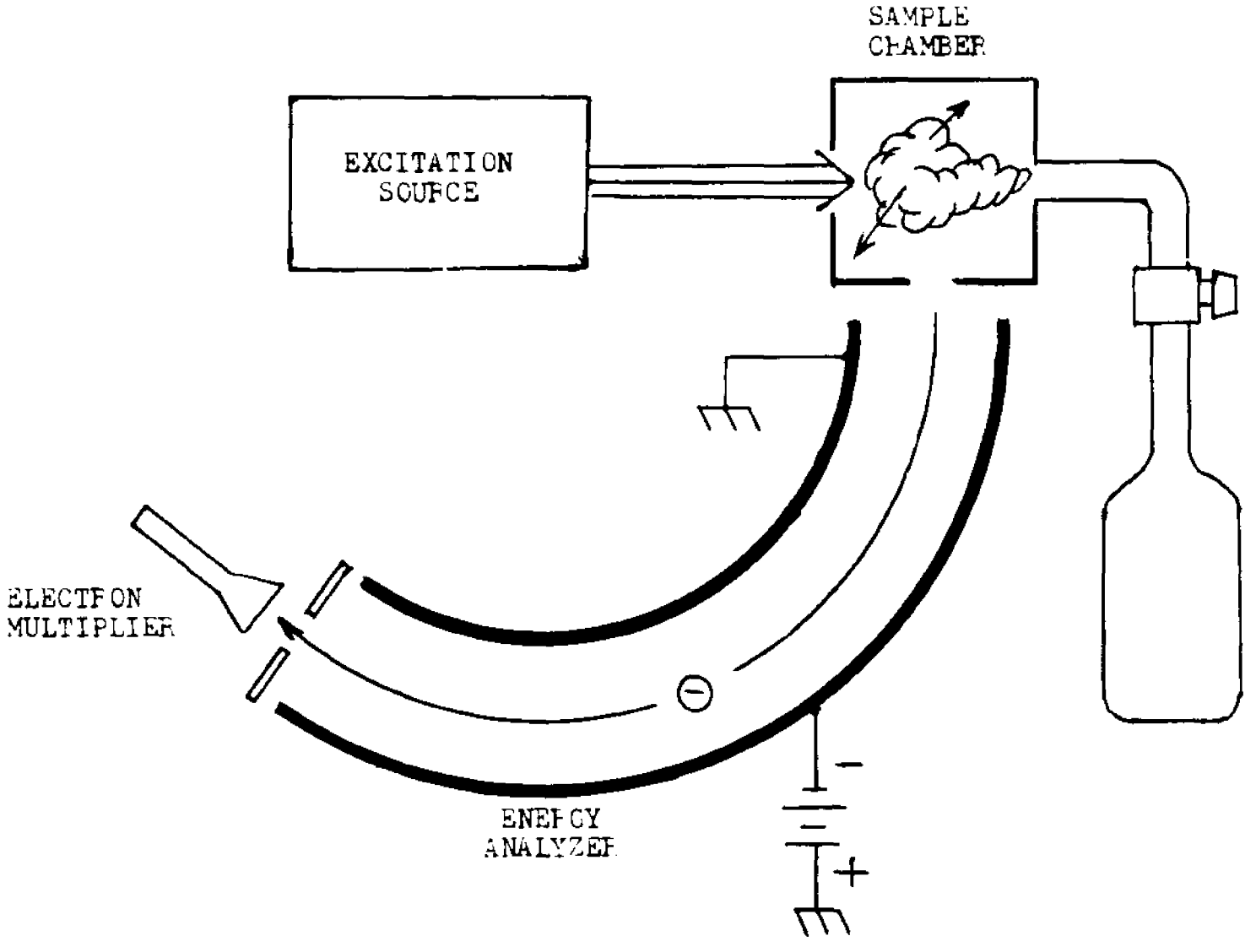

TABLE II

THE SAGA OF THE ONE PARAMETER EXPERIMENT

Cast of characters: Excitation Source ES (electron, photon, or metastable atom)
sample molecule M
Energy Analyzer
Electron detector

Opening scene: $ES + M \longrightarrow M^* + e$
The electron is transmitted by the analyzer and detected.
(chorus of theme song)

THE END

where g is the fraction of all electrons within the analyzer energy window ΔE, and where f_e is the fraction of electrons within the energy window which are transmitted (determined by the focussing properties of the analyzer, see Chap. 3).

As techniques of energy analysis and data processing have become more refined, there has been an expanding interest in two parameter coincidence experiments. Although these experiments are inherently more difficult to perform and provide much lower rates of data collection, they are the only unambiguous means of examining the fates of excited ions and molecules.

Electron-Ion Coincidence Spectroscopy

Considering the extensive work done in electron impact and photoionization mass spectrometry, it is curious how poorly understood are the ionization and fragmentation processes of molecules. Since the mass spectrum of a compound contains the cumulative ion fragmentation products of all possible excitations and ionizations of the molecule, it is virtually impossible to infer the ion products resulting from dissociation of a particular parent ion state. Although a theoretical analysis of the fragmentation of ions is possible using the Quasi-equilibrium Theory of Mass Spectra[76,77], agreement with experimental data is often only semiquantitative, and in some cases, glaring discrepancies exist.

Whether electron impact or photoionization is employed, the processes of ionization and fragmentation may be visualized as occurring in two distinct successive steps. Initially, molecules are ionized into various excited states of the parent ion, which then subsequently

undergo fragmentation into the various ions characteristic of the mass spectrum of the compound.

Once a molecule is ionized, the dissociation into fragments may be direct, whereby the breaking of a specific bond within the molecule follows as an immediate consequence of the removal of a strongly bonding electron. An alternate fragmentation process is predissociation, in which the nature of the original molecular orbital from which ionization has occurred has little bearing upon the fragmentation products; even ionization of "non-bonding" lone-pair electrons may well result in dissociation. Predissociation occurs when the electronic excitation energy of the parent ion is converted into vibrational energy, which will become redistributed until eventually sufficient vibrational energy is localized within one portion of the ion to repture a bond.

By the use of photoelectron-photoion coincidence spectroscopy, the fragmentation products of a particular ion state can be directly observed. In essence, the technique allows the experimenter to select one particular ionization process, and then observe the resulting mass spectrum. Photoelectron-photoion coincidence spectroscopy has allowed ion fragmentation pathways to be determined for CO_2[78], SO_2[79], CS_2[80], N_2O[81], COS[81], CH_4[82], C_2H_6[82], CH_2Cl_2[83], CH_2Br_2[84], CH_2I_2[84], C_2F_6[85] and C_6H_6[86]. For these compounds then, the origin of each ion in the photoionization mass spectrum has been completely determined.

Electron impact on molecules, as well as forming the same parent ion states as are encountered in photoionization, will lead to excited neutral molecules as well, which if sufficiently excited may then undergo

autoionization. Therefore, a full understanding of electron-impact mass spectra will require autoionization coincidence experiments to be performed, although as of this writing, this type of experiment has yet to be successfully undertaken. The characteristics and limitations of such a technique would be very similar to photoelectron-photoion coincidence spectroscopy, which although difficult to conduct, has been demonstrated to be a viable technique.

Limitations of Photoelectron-Photoion Coincidence Spectroscopy

The basic experimental apparatus for a photoelectron-photoion coincidence experiment is depicted in Fig. (26). As a source for the photoionization of the sample gas within th ionization region, monochromatic radiation (usually HeI radiation of 21.21 eV energy) is commonly used. Some experiments[82,84] however have utilized a continuous source of radiation with a vacuum UV monochromator, providing a monochromatic source of variable energy. Although the use of a monochromator results in substantial attenuation of the photon intensity (and adds considerable cost), it nonetheless allows the photoejection of electrons of low kinetic energy. Since the collection efficiency of energy analyzers is inherently superior for electrons originating with low kinetic energy (see Chap. 3), a gain in data collection rate may be realized by the use of a variable energy source.

In any event, the photoelectrons produced enter an energy analyzer, which transmits a fraction, f_e, of electrons of a preselected energy (corresponding to a particular ionization process of interest). Upon detection of an electron, indicating that the selected ionization process

Figure(26)
Schematic Diagram of a Photoelectron-Photoion Coincidence Experiment

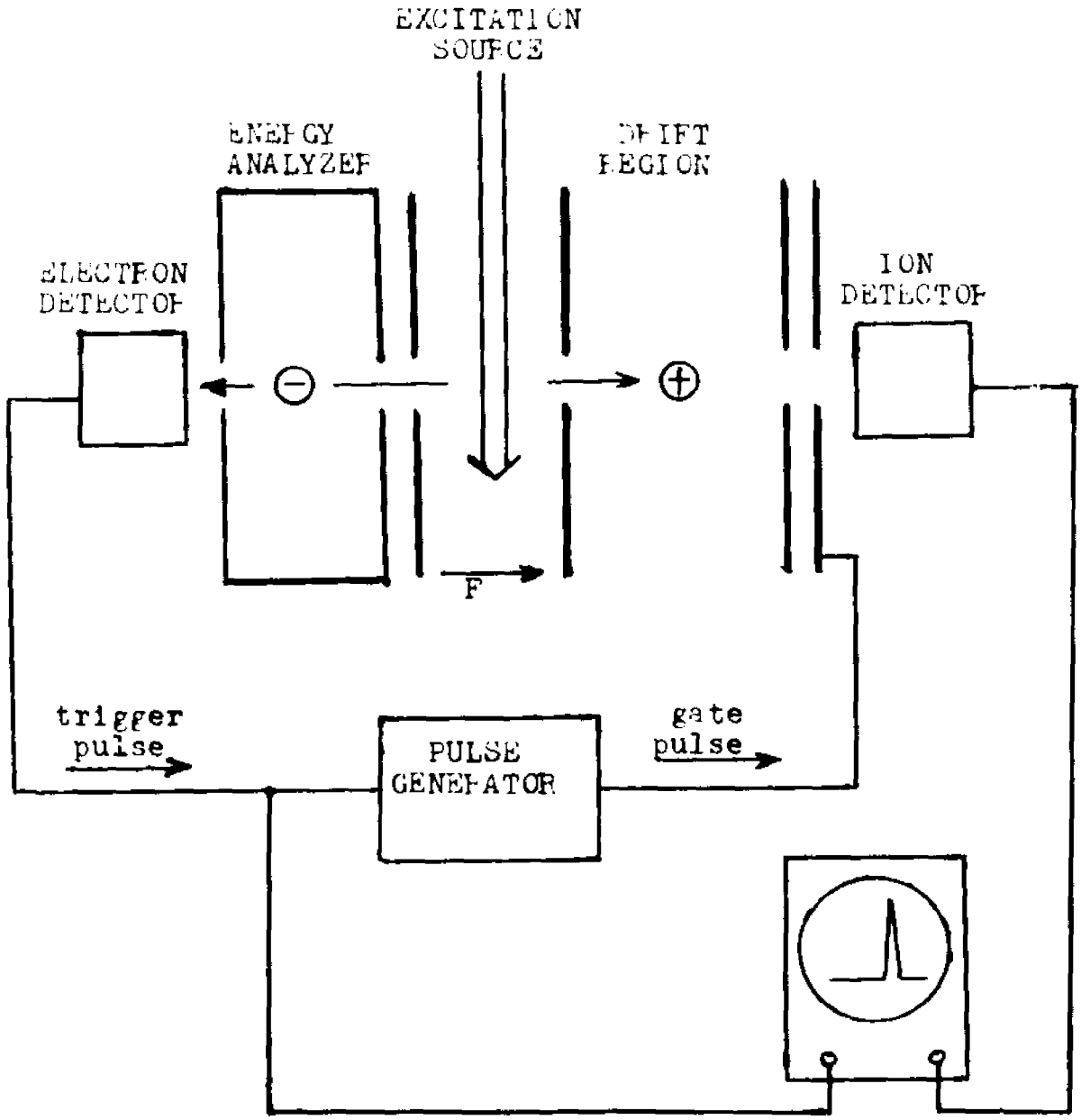

TABLE III

PHOTOELECTRON-PHOTOION COINCIDENCE SPECTROSCOPY:
A TALE OF TWO PARAMETERS

Opening scene $h\nu + M \longrightarrow M^+ + e$

$M^+ \longrightarrow M_1^+ + M_2$

Scene 2

Electron multiplier: An electron of energy E has been detected. Alert the kingdom! (sound trumpets)

Pause (time-of-flight of ion)

Ion detector: An ion has been detected, just about the time when an ion of mass M_1 is expected to arrive.

Scene 3

Experimenter: Can we be sure that the ion detected really resulted from the ionization in question, or perhaps was totally uninvolved and by chance stumbled into the detector while we expected ion M_1^+.

Colleague: Indeed, we must examine the outcome of many ionizations before we can be sure of our conclusion.

(Curtain closes)

the end

has occurred, the arrival of the resulting ion is anticipated at the ion detector.

Within the ionization region, a constant electric field F will accelerate the resulting ion out of the ionization region, whereupon it will drift toward the ion detector, the expected arrival time depending upon the mass of the ion.

Consider an ion of mass M resulting from the detected photoionization process. Since the time of the ionization process is specified almost exactly by the detection of the photoelectron (the time-of-flight of the electron through the analyzer is usually negligible, and can be compensated for), it is tempting to believe that the arrival time of an ion of mass M could be predicted exactly. However, ions formed with initial velocities in the direction of the accelerating field will arrive at an earlier time than those initially moving opposite the field, which must be retarded to a standstill and then reaccelerated. Consequently, as a result of the initial kinetic energy E_I of the ion, the arrival time of an ion of mass M cannot be specified exactly, but only within a time range t_m, the "turnaround time" of an ion, where[87]

$$t_m = (2.9 \times 10^{-6})(ME_I)/F \text{ seconds} \qquad \text{(VI-2)}$$

While parent ions are formed only with thermal energy (averaging about 0.040 eV at room temperature), fragment ion kinetic energies are often considerable, averaging up to one eV.

The uncertainty in the exact arrival time of the ion of mass M will lead to an inherent limitation of the instrument to distinguish between the ion formed as a result of the detected photoionization, and any other ion which by random chance happens to strike the ion detector during the "time

window", t_m.[88]

Consider the case where I ionizations occur each second in the ionization region, of which only a fraction $f_e(g\Delta E)$ of the photoelectrons enter the analyzer with the proper orientation and are of the proper energy to be transmitted and detected. Therefore, $If_e g\Delta E$ electrons are detected each second and trigger a time-of-flight mass spectrum of the resulting ion.

The detection of each electron will be followed by the successful observation of the resulting ion if ideal ion collection is assumed. Of the ions resulting from the selected ionization process, a fraction p_M will be of mass M. Consequently, the number of ions of mass M detected in coincidence with photoelectrons of known energy is,

$$S = (If_e g\Delta E)p_M \qquad \text{(VI-3)}$$

However, during each time range t_m corresponding to the detection of an ion of mass M in each mass scan, It_m ions will arrive at the ion detector by random chance. These ions comprise a constant average background of "false coincidences" which will be detected during the entire duration of each time-of-flight spectrum. This background itself will present no difficulty, as it can be predicted and subtracted from the resulting spectrum. Statistical fluctuations however will inevitably be present in this background, which can neither be predicted, nor eliminated, and will constitute noise.

Such noise degrades the information content of the detected signal and can only be diminished by increasing the time period t during which data is collected. At an optimal ionization rate (such that a maximum signal

is present without saturation of the detectors) the signal/noise ratio for ions of mass M formed in coincidence with the selected ionization will be limited to a maximum value given by[89],

$$(VI-4) \qquad (S/N)_{optimal} = (f_e g \Delta E . p_M^2/t_m)^{\frac{1}{2}} t^{\frac{1}{2}}$$

The signal/noise ratio determines the actual rate at which useful data of real coincidences is collected, and may be thought of as arising from an effective signal, S_{eff}, consisting only of real coincidences. As all ions resulting from the selected ionization process will be detected during the time-of-flight mass scan, the total rate at which data is accummulated will be the summation of the effective signal, S_{eff}, for all ions. By analogy with Eq. (I-3), the effective rate of data collection for all ions detected in coincidence with the selected photoionization is:

$$(VI-5) \qquad S_{eff} = N_{eff} \cdot f_e g \Delta E \quad \text{coincidences/seconds}$$

$$\text{Where } N_{eff} = \sum_{\substack{\text{all} \\ \text{ions}}} p_M^2/t_m$$

The effective rate of ionizations per second, N_{eff}, will depend primarily upon the initial kinetic energy of the ions, the width of the ionization region, and the electric field within the ionization region. Typically, N_{eff} will be of the order of 10^5 ionizations/second, as compared to a typical ionization rate in a one parameter experiment of about 10^8 ionizations/second.

The most convenient way to increase N_{eff}, and hence the rate of data accummulation is by increasing the electric field within the ionization region, and in doing so, decreasing the ion "turnaround time".

However, this electric field results in an energy spread of the photoelectrons, and so, limits the electron energy resolution which may be achieved. A higher data collection rate resulting from an increase of the electric field F is achieved only with a concommitent sacrifice of electron energy resolution. Once again, a fundamental trade-off between the attainable signal count rate and resolution becomes apparent.

As a consequence of the inherently poor rate of data collection achieved in coincidence experiments (at reasonable electron energy resolution), time periods of days are often required to collect data and achieve high signal/noise ratios. In the future, several possibilities may be exploited to decrease the required data collection time. Higher rates of data collection may be achieved (with the same resolution) by restricting the width of the ionization region (although this will only be successful to a limited extent, determined by the brightness of the ionizing radiation source), making use of high transmission analyzers, or incorporating multichannel array detectors to achieve multichannel electron energy analysis. In particular, the increasing availability, at reasonable cost, of sophisticated data handling electtonics may be expected to result in improved resolution and data collection rates.

Other similar coincidence experiments have been performed to analyze the fragmentation of multiply charged ions[90], the kinetic energies of fragment ions from known initial parent ion states[79,80,91], and the lifetimes of excited ion states[92]. A summary of coincidence electron spectroscopy experiments performed to date, and potential applications of coincidence experiments will soon be published[93].

REFERENCES

1 W.G. Wolber and B.D. Kettke, Rev. Scient. Instr., 41 (1970) 724

2 P.W. Graves, B.D. Kettke, N.D. Krym and W.G. Wolber, Technical Applications Note 6902, Bendix Research Labs, Southfield, Mich. 48075 (1969)

3 J.E. Rowe, S.B. Christman and R.D. Plummer, Rev. Scient. Instr., 42 (1971) 1733

4 RCA Photomultiplier Manual, RCA Electr. Components Div., Harrison, N.J. pp 56-76

5 Yisrael A Isaacson, Zenowij Majuk, Marion A. Brisk, Martin E. Gellender and Arthur D. Baker, JACS, 97 (1975) 6603

6 A.D. Baker, M. Brisk and M. Gellender, J. Electron Spectrosc., 3 (1974) 227

7 G.A. Harrower, Rev. Scient. Instr., 26 (1955) 850

8 A.L. Hughes and V. Rojansky, Phys. Rev., 34 (1929) 284

9 E.M. Purcell, Phys. Rev., 54 (1938) 818

10 H.Z. Sar-el, Rev. Scient. Instr., 38 (1967) 1210

11 H.Z. Sar-el, Rev. Scient. Instr., 42 (1971) 1601

12 G.M. Renfro and H.J. Fischbeck, Rev. Scient. Instr. 46 (1975) 670 Discusses the effect of fringing in cylindrical mirror analyzers.

13 D.W. Turner, C. Baker, A.D. Baker and C.R. Brundle, Molecular Photoelectron Spectroscopy, Wiley (1970)

14 K.D. Sevier, Low Energy Electron Spectrometry, Wiley (1972) Chaps. 2&3

15 M.E. Gellender and A.D. Baker, J. Electron Spectrosc., 4 (1974) 249 (see Appendix 1)

16 H. Frotzheim, H. Ibach and S. Lehwald, Rev. Scient. Instr., 46 (1975) 1325

17 H.Z. Sar-el, Rev. Scient. Instr., 41 (1970) 561

18 D.W.O. Heddle, J. Phys. E (Scient. Instr.), 4 (1971) 589

19 H. Hafner, J. Arol Simpson and C.E. Kuyatt, Rev. Scient. Instr., 39 (1968) 33

20 C.E. Kuyatt and J. Arol Simpson, Rev. Scient. Instr., 38 (1967) 103

21 J. Arol Simpson, Rev. Scient. Instr., 35 (1964) 1698

22 J. Arol Simpson, Rev. Scient. Instr., 32 (1961) 1283

23 J.D. Lee, Rev. Scient. Instr., 44 (1973) 893

24 J.C. Helmer, Amer. J. Phys., 34 (1966) 222

25 private communication and notes of C.E. Kuyatt (U.S. Nat'l Bur. Stds.) 1972

26 Tomas Baer, W.B. Peatman and E.W. Schlag, Chem. Phys. Letters, 4 (1969) 243

27 J.C. Helmer and N.H. Weichert, Appl. Phys. Lett., 13 (1968) 266

28 P. Marmet, Rev. Scient. Instr., 44 (1973) 67

29 K. Siegbahn, D. Hammond, K. Fellner-Feldig and E.F. Barnett, Science, 176 (1972) 245

30 U. Gelius, E. Basiler, S. Svenson, T. Bergmark and K. Siegbahn, J. Electron Spectrosc., 2 (1973) 405

31 Operations and Maintenance Manual 994039, Dupont 650 Electron Spectrometer, Instr. Prod. Div., E.I. Dupont de Nemoirs & Co., Wilmington, Del. 19898

32 H. Moestue, Rev. Scient. Instr., 44 (1973) 1709

33 J.R. Pierce, Theory and Design of Electron Beams, Van Nostrand (1954)

34 V.K. Zworykin, Electron Optics and the Electron Microscope, John Wiley (1945)

35 P.W. Hawkes, Electron Optics and Electron Microscopy Barnes and Noble (1972)

36 O. Klemperer and M.E. Barnett, Electron Optics, Cambridge (1971)

37 P. Grivet, Electron Optics, Pergamon Press (1965)

38 A. Septier (ed.), Focussing of Charged Particles, Vol. II, Academic Press (1967)

39 P. Dahl, Introduction to Electron and Ion Optics, Academic Press (1973)

40 O. Klemperer, Electron Optics, Univ. Press (1953)

41 B. Paszkowski, Electron Optics, Elsevier (1968)

42 F.H. Read, J. Phys. E (Scient. Instr.), 2 (1969) 679

43 D.W.O. Heddle, J. Phys. E (Scient. Instr.), 2 (1969) 1046

44 M.V. Kurepa, M.D. Tasic and J.M. Kurepa, J. Phys. E (Scient. Instr.), 7 (1974) 940

45 K. Siegbahn et al, ESCA Applied to Free Molecules, North Holland Publ. Co. (1969)

46 William Ervin Moddeman, PhD thesis (Auger Spectra of Simple Gaseous Molecules), Univ. of Tennessee/Oak Ridge Nat'l Lab. (Sept. 1970)

47 N. Ostojic and Z. Sternberg, Chromatographia, 7 (1974) 3

48 J.T.S. Schmermund and David C. Locke, Analytical Letters, 8 (1975) 611

49 F.P. Lossing and Ikuzo Tanaka, J. Chem. Phys., 25 (1956) 1031
R.F. Herzog and F.F. Marmo, J. Chem. Phys., 27 (1957) 1202

50 N.W. Reid, Int. J. Mass Spectrom. Ion Phys., 6 (1971) 1
R.M. Elliot, Ion Sources, chap 4 in Mass Spectrometry (ed. C.A. McDowell) McGraw Hill (1963)

51 A.D. MacDonald, Microwave Breakdown in Gases, Wiley (1966)

52 Sanborn C. Brown, Introduction to Electrical Discharges in Gases, Wiley (1966)

53 Essam Nasser, Fundamentals of Gaseous Ionization and Plasma Electronics, Wiley Interscience (1971)

54 F.M. Penning, Electrical Discharges in Gases, MacMillan (1957)

55 G.F. Weston, Cold Cathode Glow Discharge Tubes, Iliffe Books Ltd., London (1968)

56 R.T. Poole, J. Liesegang, R.C.G. Leakey and J.G. Jenkin, J. Electron Spectrosc., 5 (1974) 773

57 F. Burger and J.P. Maier, J. Electron Spectrosc., 5 (1974) 783

58 C.Y. Bartholomew, G. Cassady and A.R. LaPadula, J. Applied Phys., 33 (1962) 230

59 C.Y. Bartholomew and A.R. LaPadula, J. Applied Phys., 35 (1964) 2570

60 D. Rosenberg and G.K. Wehner, J. Applied Phys., 33 (1962) 1842

61 N. Laegrid and G.K. Wehner, J. Applied Phys., 32 (1961) 365

62 G.K. Wehner, Phys. Rev., 108 (1957) 35

63 R. Gordon Jr., R.E. Rebbert and P. Ausloos, NBS Technical Note 496 (Oct. 1969). This note was no longer available from the U.S. Supt. of Documents as of June 1975.

64 F.C. Fehsenfeld, K.M. Evensen and H.P. Broida, Rev. Scient. Instr., 36 (1965) 294

65 James A.R. Samson, Techniques of Vacuum Ultraviolet Spectroscopy, John Wiley (1967)

66 W.E. Bell, A.L. Bloom and J. Lynch, Rev. Scient. Instr., 32 (1961) 688

67 R.G. Bower, Rev. Scient. Instr., 12 (1961) 1356

68 M.H. Greenblatt, Rev. Scient. Instr., 29 (1958) 738

69 personnal communication with Russ Huebener of Argonne Nat'l. Labs, Argonne, Ill.

70 The author was made aware of bonded thoria filiments after a discussion with Dave Spence of Argonne Nat'l. Labs revealed that such cathodes have been used for negative ion resonance experiments.

71 M.E. Haine and D. Linder, High Brightness Electron Guns, Chap 2.1 in Focussing of Charged Particles Vol. I (ed. A. Septier) Academic Press (1967) pp. 233-250

72 J. Arol Simpson, Electron Guns, Chap 1.1.5. in Methods of Experimental Physics 4A (ed. L. Marton), Academic Press (1967) p. 84-95

73 George R. Brewer, High Intensity Electron Guns, Chap. 3.2 in Focussing of Charged Particles Vol. II (ed. A. Septier) Academic Press (1967)

74 J.R. Pierce, Theory and Design of Electron Beams, Chap. X, Van Nostrand (1954)

75 J.A. Simpson and C.E. Kuyatt, Rev. Scient. Instr., 34 (1963) 265

76 A.L. Wahrhaftig, Theory of Mass Spectra, in MTP Int. Rev. of Science (Phys. Chem. Series One)(ed. A. Maccoll) Vol. 5, Univ. Park Press, Balt. (1972) p. 1

77 H.M. Rosenstock and M. Krause, Advances in Mass Spectrosc., 2 (1963) 251

78 J.H.D. Eland, Int. J. Mass Spectrom. Ion Phys, 9 (1972) 3917

79 B. Brehm, J.H.D. Eland, R. Frey and A. Küstler, Int. J. Mass Spectrom. Ion Phys., 12 (1973) 197

80 B. Brehm, J.H.D. Eland, R. Frey and A. Küstler, Int. J. Mass Spectrom. Ion Phys., 12 (1973) 213

81 J.H.D. Eland, Int. J. Mass Spectrom. Ion Phys., 12 (1973) 389

82 R. Stockbauer, J. Chem. Phys., 58 (1973) 3800

83 C.J. Danby and J.H.D. Eland, Int. J. Mass Spectrom. Ion Phys., 8 (1972) 153

84 B. Tsai, T. Baer, A.S. werner and S.F. Lin, J. Phys. Chem., 79(1975)570

85 I.G. Simm, C.J. Danby and J.H.D. Eland, Int. J. Mass Spectrom. Ion Phys., 14 (1974) 285

86 J.H.D. Eland, Int. J. Mass Spectrom. Ion Phys., 13 (1974) 457

87 A. Harvey, M-De-L.F. Montiero and R.I. Reid, Int. J. Mass Spectrom. Ion Phys., 4 (1970) 365

88 J.H.D. Eland, Int. J. Mass Spectrom. Ion Phys., 8 (1972) 143

89 M.E. Gellender and A.D. Baker, Int. J. Mass Spectrom. Ion Phys., 17 (1975) 1

90 K.E. McCulloh, T.E. Sharp and H.M. Rosenstock, J. Chem. Phys., 42 (1965) 3501

91 B. Brehm, R. Frey, A. Küstler and J.H.D. Eland, Int. J. Mass Spectrom. Ion Phys., 13 (1974) 251

92 M. Block and D.W. Turner, Chem. Phys. Letters, 30 (1975) 344

93 M.E. Gellender and A.D. Baker, Two Parameter Coincidence Experiments, in Electron Spectroscopy: Theory, Techniques and Applications (ed. C.R. Brundle and A.D. Baker) Academic Press, to be published.